SENSUM

Framework to integrate Space-based and in-situ sENSing for dynamic vUlnerability and recovery Monitoring

FP7-SPACE-2012-1 Collaborative Project **312972**

Deliverable

Deliverable	Supervised/Unsupervised change detection
D2.6	

Workpackage	2	**Status (F=Final, D=Draft)**	D
File name	D2.6 supervised_unsupervised_change_detection		
Dissemination Level (PU=Public; RE=Restricted; CO=Confidential)		PU	

Document Control Page

Version	Date	Comments
1	10/07/2014	First draft
2	12/11/14	Reviews by EUCENTRE and GFZ
3	14/11/14	Final draft by UCAM and EUCENTRE
4	16/12/14	Final check by GFZ (KF)

Authors	
Name	**Institution**
Dilkushi de Alwis Pitts	UCAM
Daniele De Vecchi	EUCENTRE
Mostapha Harb	EUCENTRE
Emily So	UCAM
Fabio Dell'Acqua	EUCENTRE

Deliverable Leader	**Name**	Emily So
	Institution	UCAM
Keywords	Change detection; co-registration	

Table of Contents

Illustration Index

Glossary of Terms

GFZ	German Research Centre for Geosciences, DE
EUCENTRE	European Centre for Training and Research in Earthquake Engineering, IT
DLR	German Aerospace Centre, DE
NGI	Norwegian Geotechnical Institute, NO
UCAM	University of Cambridge, UK
CAIAG	Central Asian Institute for Applied Geosciences, KG
IGEES	Institute for Geology and Earthquake Engineering, TJ
ICAT	ImageCat Ltd., UK
EC	European Commission
WP	Workpackage
DoW	Description of Work
DEM	Digital Elevation Model
GCP	Ground Control Point
OpenCV	Open Computer Vision
SIFT	Scale Invariant Feature Transform
SURF	Speeded-Up Robust Features
BRIEF	Binary Robust Independent Elementary Features

Executive Summary

The aim of this deliverable is to provide an overview of the state of the art in change detection techniques and a critique of what could be programmed to derive SENSUM products. It is the product of the collaboration between UCAM and EUCENTRE. The document includes as a necessary requirement a discussion about a proposed technique for co-registration. Since change detection techniques require an assessment of a series of images and the basic process involves comparing and contrasting the similarities and differences to essentially spot changes, co-registration is the first step. This ensures that the user is comparing like for like. The developed programs would then be used on remotely sensed images for applications in vulnerability assessment and post-disaster recovery assessment and monitoring. One key criterion is to develop semi-automated and automated techniques.

A series of available techniques are presented along with the advantages and disadvantages of each method. The descriptions of the implemented methods are included in the deliverable D2.7 ”Software Package SW2.3”.

In reviewing the available change detection techniques, the focus was on ways to exploit medium resolution imagery such as Landsat due to its free-to-use license and since there is a rich historical coverage arising from this satellite series.

Regarding the change detection techniques with high resolution images, this was also examined and a recovery specific change detection index is discussed in the report.

Introduction

The aim of this report is to summarise the state of the art in change detection techniques for use on medium- and high-resolution remotely sensed imagery. The core two applications of SENSUM products are in vulnerability assessments (WP2) and in post-disaster recovery assessment and monitoring (WP5). Both of these applications could make use of change detection techniques to monitor changes to the built environment through time, first by examining the building inventory, mix of typology and distribution, and then, in the case of recovery monitoring, document the spatial and quantitative changes through time to review how far the affected communities have recovered.

In collaboration, UCAM and EUCENTRE have reviewed change detection and co-registration methods and have in this report submitted a proposed method for use in SENSUM. The methods chosen are based on the state of the art, and have been evaluated to suit the goals of the project, that is to assess and analyse the urban built environment, although these techniques can also be adapted to extract other physical outputs.

At the core of any change detection technique is the need to process a time series of remote sensing imagery together. In order to ensure the imageries are not biased by the sensors and physical conditions when the images are taken (sun position, illumination, shadows, etc.), a set of corrections must be made to the images to co-register them. Such techniques are reviewed in the next section. The report will then present the techniques available for the temporal analyses of medium- and high-resolution images. The report will conclude with suggestions for their implementation into the programmed algorithms outlined in deliverable D2.7 ”Software Package SW2.3”, with a brief description of how these techniques can be used for SENSUM applications in WP4 and WP5.

Co-registration

Image registration is the process of overlaying two or more images of the same scene taken at different times, from different viewpoints and/or from different sensors (*Zitova and Flusser, 2003*). The specific case analysed in this deliverable is related to medium resolution imagery and Landsat in particular. A brief introduction is given below to Landsat's main characteristics, while the rest if this section is related to the techniques outlined in the literature and the approach developed by the EUCENTRE team.

1. Landsat features

The main issue in the utilization of images from different dates is represented by distortions due to changes affecting the acquisition system, such as sensor degradation, atmosphere, illumination and the sun's position. These challenges are typically solved with geometric and radiometric corrections. The focus of this document is on the first topic, while the latter can partially be compensated with by season-matching imagery (meaning images acquired almost in the same season).

According to (*USGS, 2014)*, three correction levels are available for Landsat products:

- *Level 1T – precision and terrain correction*
  Standard correction level where Ground Control Points (GCPs) and Digital Elevation Models (DEMs) are used to increase the geometric accuracy.
- *Level 1Gt – systematic terrain correction*
  Correction available only in certain areas where there is lack of GCPs (e.g., Landsat 7 images of Antarctica); DEMs only are used to perform the correction.
- *Level 1G – systematic correction*
  Products with the lowest geometric accuracy due to the lack of GCPs and DEMs. The ephemeris is used to assign the position.

An ephemeris gives the satellite's position and velocity in the sky at a given time. In the Landsat case, the ephemeris is estimated using tracking data (*USGS, 2014*).

The band-to-band accuracy shows a band average root mean square of$\pm 0.10$of a 30m pixel for Landsat 7 products. Regarding the image-to-image correction, Landsat 7 products should guarantee an accuracy around 7.3 meters (*USGS, 2014*). Unfortunately, since 2003, images from Landsat 7 are suffering a scan line error with the consequent impairment of the data. Landsat 5 meanwhile continued its acquisition campaign filling the gaps, but with the drawback of lower geometric accuracy in respect of the Landsat 7. In particular, several L5 products are released as L1G datasets (lowest geometric accuracy available) but they cannot be discarded a-priori: the presence of clouds and the need for season-matching data can force the use of this kind of imagery within the processing chain.

2. Geometric correction

According to (*Goward et al., 2001*), three different types of geometric correction can be taken into account: (1) band-to-band, (2) image-to-image and (3) image-to-map.

As a mission of the SENSUM project is to provide monitoring tools for vulnerability- and recovery-mapping, a consistent and rich dataset is therefore mandatory. Image-to-image registration methods represented the main focus of the literature review with the final goal being to have geographically-matching data through the years.

The main methods available are:

- Manual detection and matching
- Feature-based
- Area-based

A brief explanation is provided for each one.

Manual detection and matching

A well-known solution for image registration is the manual definition of ground control points where reference and target images are compared and analysed by an end-user. The typical outcome of the procedure is a set of corresponding key-points between a reference and a target image. The selected points are successively used to determine the transformation-related equation.
Common guidelines for the points' selection suggest the use of stable features like cross-roads instead of unstable/changing features like water bodies.
The advantage of manual registration is the high precision and stability; disadvantages are mostly related to the time consumption and the necessity of a trained end-user.

Feature-based techniques

This approach is based on the extraction of significant features from the input images, for example blobs, corners or line intersections. The most famous algorithms for this task are already implemented and included in the OpenCV library (Open Computer Vision[1]).
Feature-based techniques consist of three common steps:

1. *Feature Detection*: distinctive objects like edges and corners are automatically selected;
2. *Feature Description*: every key-point extracted with the previous step is labelled according to the surroundings pixels. This step is necessary to distinguish among different points and obtain better matchings;
3. *Feature matching*: key-points and associated labels from an image are compared to all the features extracted from the other input image. The similarity measure depends on the chosen description.

Feature Detection
A solution for detection is provided by the *Scale Invariant Feature Transform* (SIFT) algorithm. It is able to extract key-points and compute descriptors from an image (*Lowe, 2004*) and is made of four main steps:

1. Scale-space extrema detection is a cascade of filters (specifically Difference of Gaussian) at different resolutions applied to find local extrema over scale and space.
2. Key-point localization is the refinement of the previously obtained potential key-points.
3. Orientation is assigned calculating the magnitude and direction of the gradient from a block of pixels around the feature of interest.

Another very powerful algorithm is called *Speeded-Up Robust Features* (SURF). It represents a simpler and faster approach for the identification and description of key-points and is proposed in *Bay et al., 2008*.
One the main advantages is represented by the usage of integral images (a complete explanation is included in the original paper) combined with the approximation of the Difference of Gaussian filters with Box filters. The orientation determination is based on wavelet responses of the pixels around the point of interest.

[1] http://opencv.org/

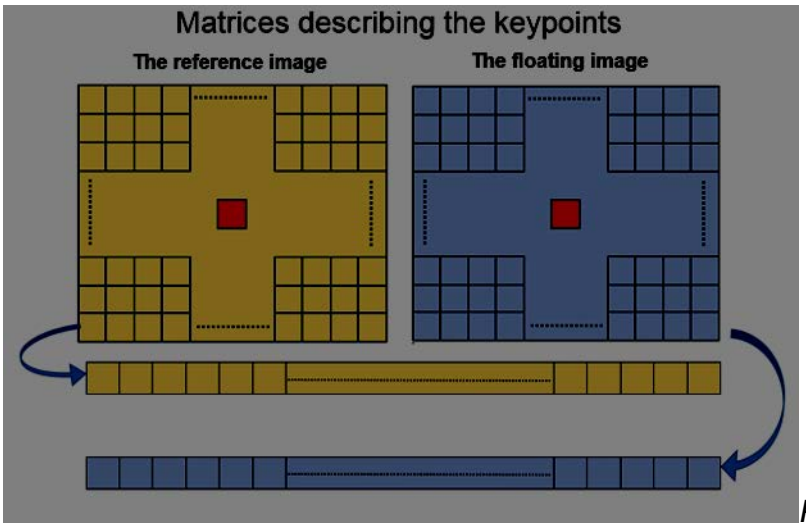

Figure 1: Example of BRIEF descriptor. Intensity of each pixel around the extracted feature is compared and a 0 or 1 value is assigned depending on the intensity difference (positive or negative.

Given the nature and robustness of the SURF algorithm, this has been used as core of the developed co-registration technique (implementation explained in the D2.7 “Software Package SW2.3” deliverable).

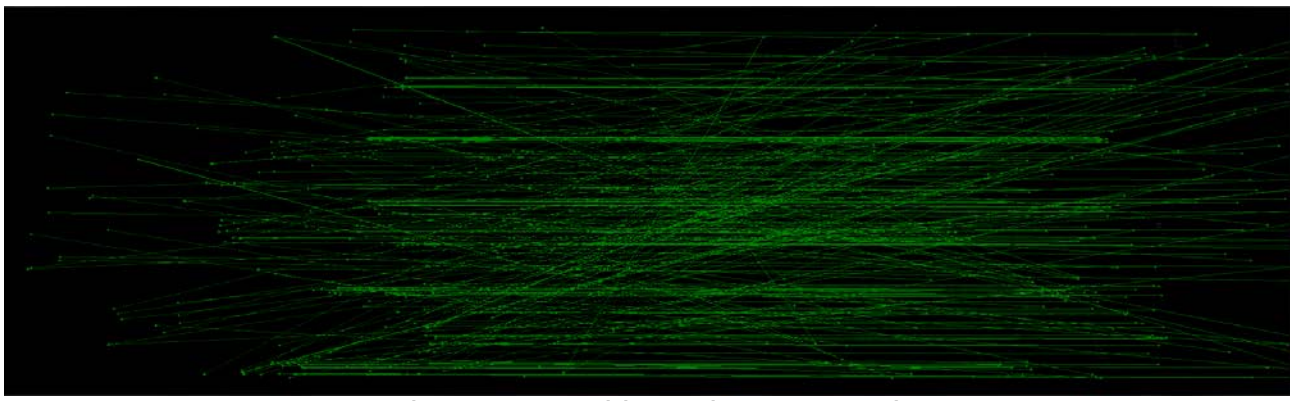

Figure 2: Matching points extracted.

Feature Description
Both SURF and SIFT algorithms provide a built-in descriptor for the extracted key-points.
The SIFT descriptor is defined by the orientation histogram computed on a 16x16 neighbourhood around the key-point. The SURF descriptor is based on wavelet responses.
However, other solutions are available for the task. For example, the BRIEF descriptor (*Calonder et al., 2010*) (also implemented in OpenCV) is fully compatible with features extracted by SURF. The defined label is a binary string computed by comparing the pixel intensity on location pairs. This descriptor is the suggested one because of the easy-to-interpret results and very simple binary metrics used.

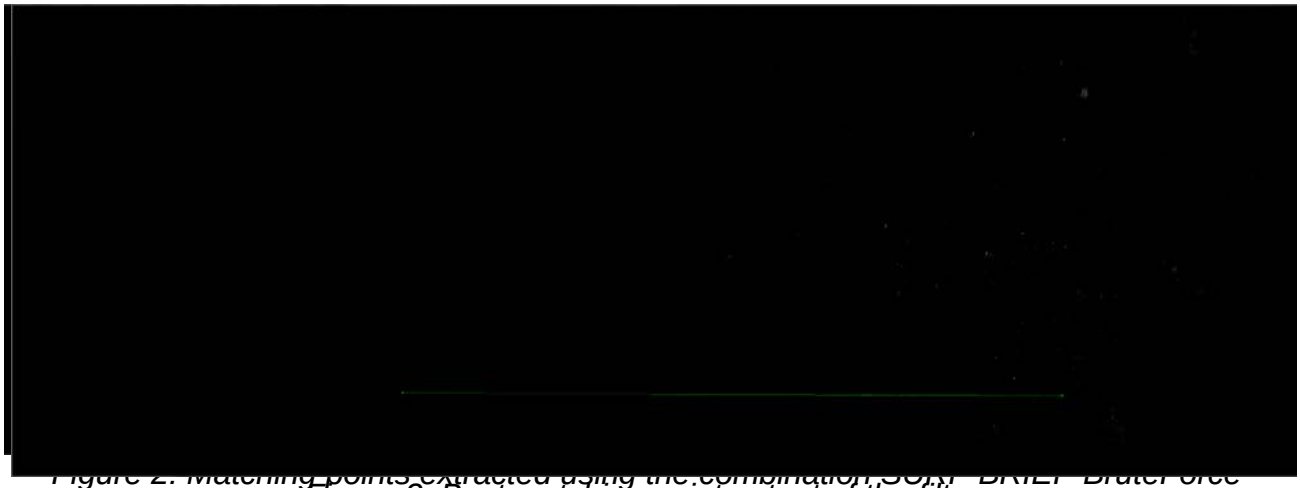

Figure 3: Best matching point output of the filters.

Figure 2: Matching points extracted using the combination SURF-BRIEF-Brute force matcher. These points cannot be directly used for correction but further filtration is necessary.

Feature Matching

The final step of a feature-based procedure consists of the comparison of all the labelled features in order to find the corresponding ones. The type of matcher depends on the selected descriptor. For example, in the case of the BRIEF descriptor, a Brute-Force matcher can be used to find the corresponding features.

The Brute-Force matcher is used to compare the label of one feature with all the other obtained descriptors: the one with the minimum distance is chosen as the corresponding one. The type of matcher can be adapted to every descriptor and consequently to its definition of distance. For example, in the BRIEF case, the metric under consideration is the hamming distance due to the binary nature of the descriptor.

The extracted matches can be ordered according to the calculated distance and further filtered.

An example of all the extracted matching points is represented by Figure 2; as the reader may notice, not all the points are correct and further filtration is needed in order to select the right ones.

Filters

Not all the matching points, as shown by Figure 2, are reliable and useful for the shift determination. Further filtering procedures must be applied in order to select just the right key-points and fix the shift.

Three filters have been designed and implemented to clean the points:

- similarity metric based on the Hamming distance;
- direction of the vector joining the two matching points defined by the slope;
- absolute distance computed as a segment length.

These filters are based on the original assumption of translational shift. This is common for medium resolution images where the acquisition angle is stable and the effect of the viewing angle is negligible. As a consequence, these filters can't be applied to other input images like high resolution images.

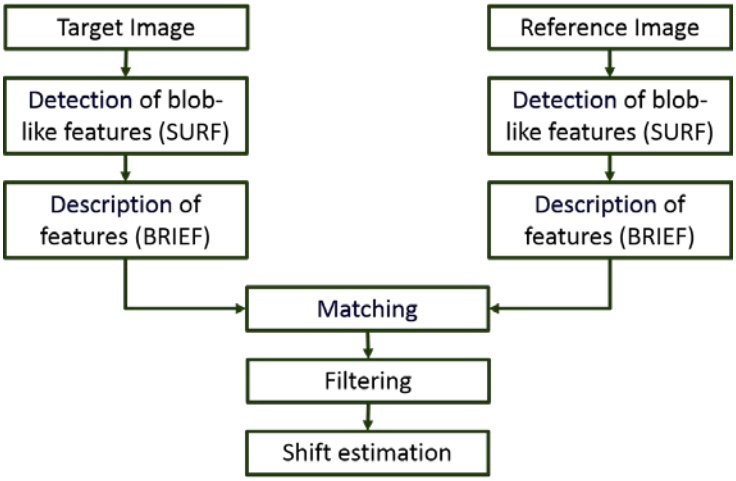

Figure 4: Feature-based workflow.

A few experiments with the feature-based approach were also performed using VHR imagery. Our results demonstrated the high potentiality of the method, but also the need to re-design from scratch all the filters due to the different distortions. The mentioned considerations and the prioritization of the extraction of vulnerability indicators from medium resolution images led to the decision to not continue the development of these tools within the current project.

Area-based techniques

Area-based techniques do not attempt to detect salient features from an image; instead, they use intensity or frequency components and their correlation properties among the analysed images.
Correlation-like methods compute the cross-correlation among rectangular windows of the images trying to find the maximum.
Fourier methods are by nature faster than correlation process. The idea is to look for the phase correlation by taking advantage of the Fourier Shift Theorem (*Tzimiropoulos et al., 2010*).

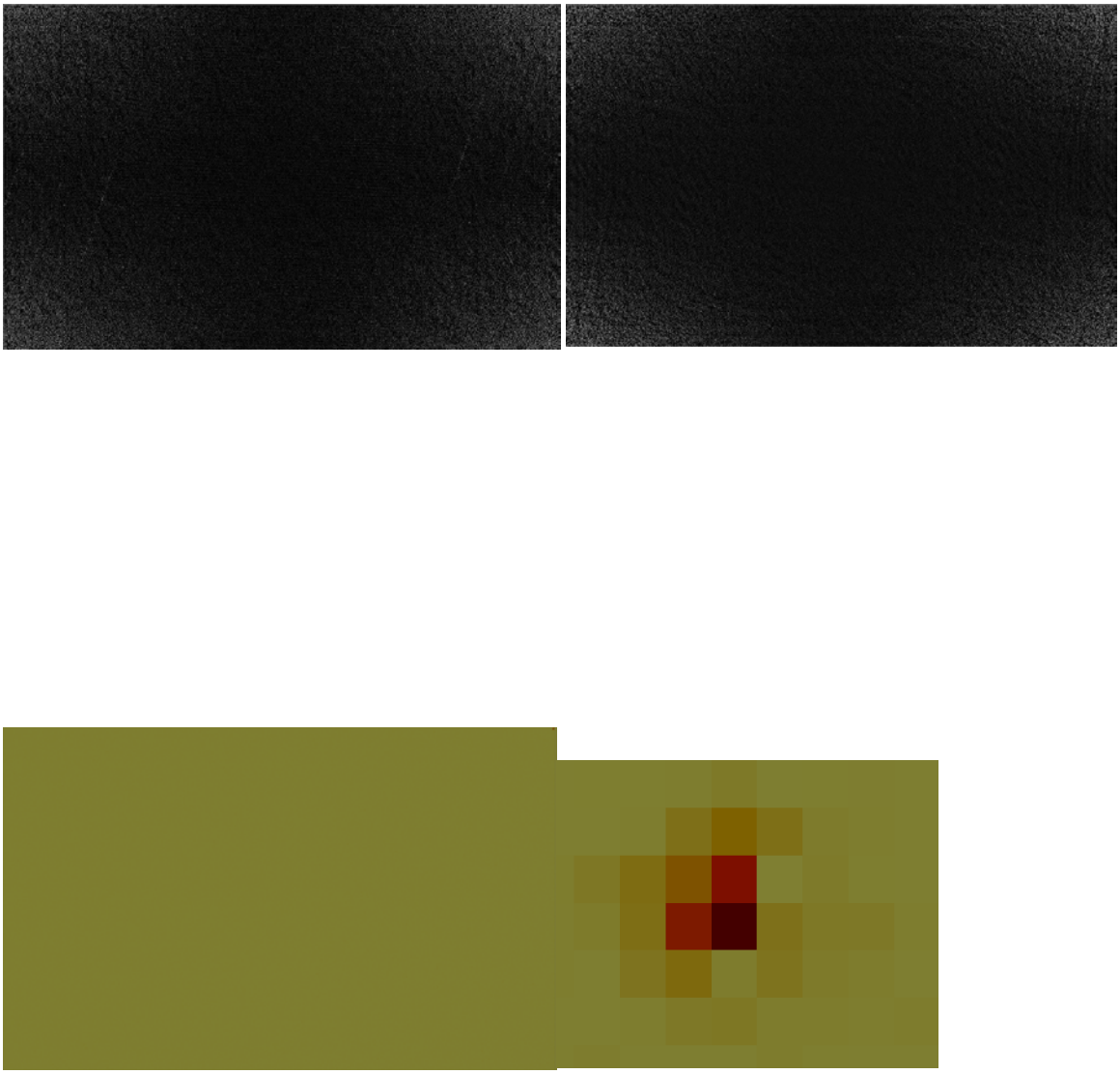

Figure 5: Example of FFT applied to the reference image (top-left). Example of FFT applied to the target image (top-right). FFT product between reference and target (bottom-left). The length of the blue arrow represents the amount of shift between reference and target (bottom-right).

Output of the FFT-based method is a single point corresponding to the peak of energy; no additional filters are needed.

Another technique coming from information theory is the use of mutual information to measure the statistical dependency of the two datasets.

For further details about all the area-based methods available in the literature, the reader is invited to refer to *Zitova and Flusser, 2003*.

Transformation

This type of mapping function corresponds to the assumed geometric deformation. In a generic case, we can assume that four types of deformation may occur:

- Translational - when the reference and target images are shifted by a certain number of pixels and the shift is constant.
- Shear - in the case of small distortion.
- Rotation - in the case where the relationship between the considered data can be modelled by an angle.
- Scale - when the images present different resolutions.

The transformation models are data-dependent and they can also be locally-defined. The latter case is more frequent in high-resolution imagery where the distortions introduced can be different in the same area of interest.

For the Landsat case considered and analysed within the project's framework, a translational-only distortion has manifested. The transformation method suggested for this case is a linear shift, applicable in different ways. One solution is an affine transformation (also implemented in OpenCV) where the transformation matrix is presented in Figure 6:

$$\begin{pmatrix} 1 & 0 & X_{shift} \\ 0 & 1 & Y_{Shift} \end{pmatrix}$$

Figure 6: Linear transformation matrix.

The first two columns are related to rotation while the third is related to translation.
Another possible solution for translational shift is to edit the geo-transform matrix associated to the image; coordinates of the starting point are modified according to the estimated shift:

$$\begin{bmatrix} Longitude_{init} & X_{resolution} & 0 \\ Latitude_{init} & Y_{resolution} & 0 \end{bmatrix} \rightarrow \begin{bmatrix} Longitute_{init} + X_{resolution} \cdot X_{shift} & 0 & X_{resolution} \\ Latitude_{init} + Y_{resolution} \cdot Y_{shift} & 0 & Y_{resolution} \end{bmatrix}$$

Figure 7: Original geo-transform matrix (left) and modifications according to the estimated shift (right).

Post-classification comparison

Change detection is by definition the capability to detect and highlight changes occurring in space and time. Remote sensing in this sense is really helpful thanks to the continuous monitoring offered by the satellite revisit period. Change detection products can be used as an input indicator for other tools produced within the SENSUM consortium, like focus maps (see products from WP3), to consequently prioritize the acquisition of in-situ image data (see deliverables D2.4 “Capture of in-situ image data” and D2.5 “Software package SW 2.2”).

One of the indicators proposed in deliverable D2.2 is related to the “Age of built-up area”. This can be interpreted as an indicator of the evolution of these areas in time and consequently of changes inside the urban extent. Data can be analysed looking for continuity along the years: input comes from the proposed unsupervised object-based methods for built-up extraction (described in deliverable D2.7) or from specific supervised classifications (different algorithms from the Orfeo Toolbox library and available with a graphic interface from the QGIS plugin). The post-classification comparison is defined as supervised or unsupervised depending on the classifier used for the single classifications.

The unsupervised method is completely automatic and relies on the user input only in the end of the process. The supervised approach is based on the definition by the end-user of built-up related classes through a training set.

3. Unsupervised methods

The unsupervised change detection technique proposed by the EUCENTRE team is based on the capability to process a series of Landsat images available for a certain area-of-interest over a given time span. The suggested time interval to consider for the process is from 3 to 5 years according to the literature (Jensen and Cowen, 1999) although this can vary considerably from area to area. Small corrections can also be applied following the common assumption that cities are growing over time (Taubenböck et al., 2011). Figure 8 shows a basic conceptual scheme of how such change detection methods work:

- all the years (and relative extractions) are input for the algorithm;
- the results are analysed in order to evaluate changes over time;
- labels are assigned based on the logic behaviour over time.

The implemented methodology makes use of the object-based outputs of the stack satellite algorithm (see deliverable D2.7 for more details). The method can be considered unsupervised because the user input is limited to the selection of the class (or classes) attributable to built-up areas from the stack satellite output. This step is, anyhow, necessary to determine the goodness of the original extraction.
Different filters have been designed and included with the aim of partially correcting errors from the original output. This task is possible thanks to the wide time span processed.

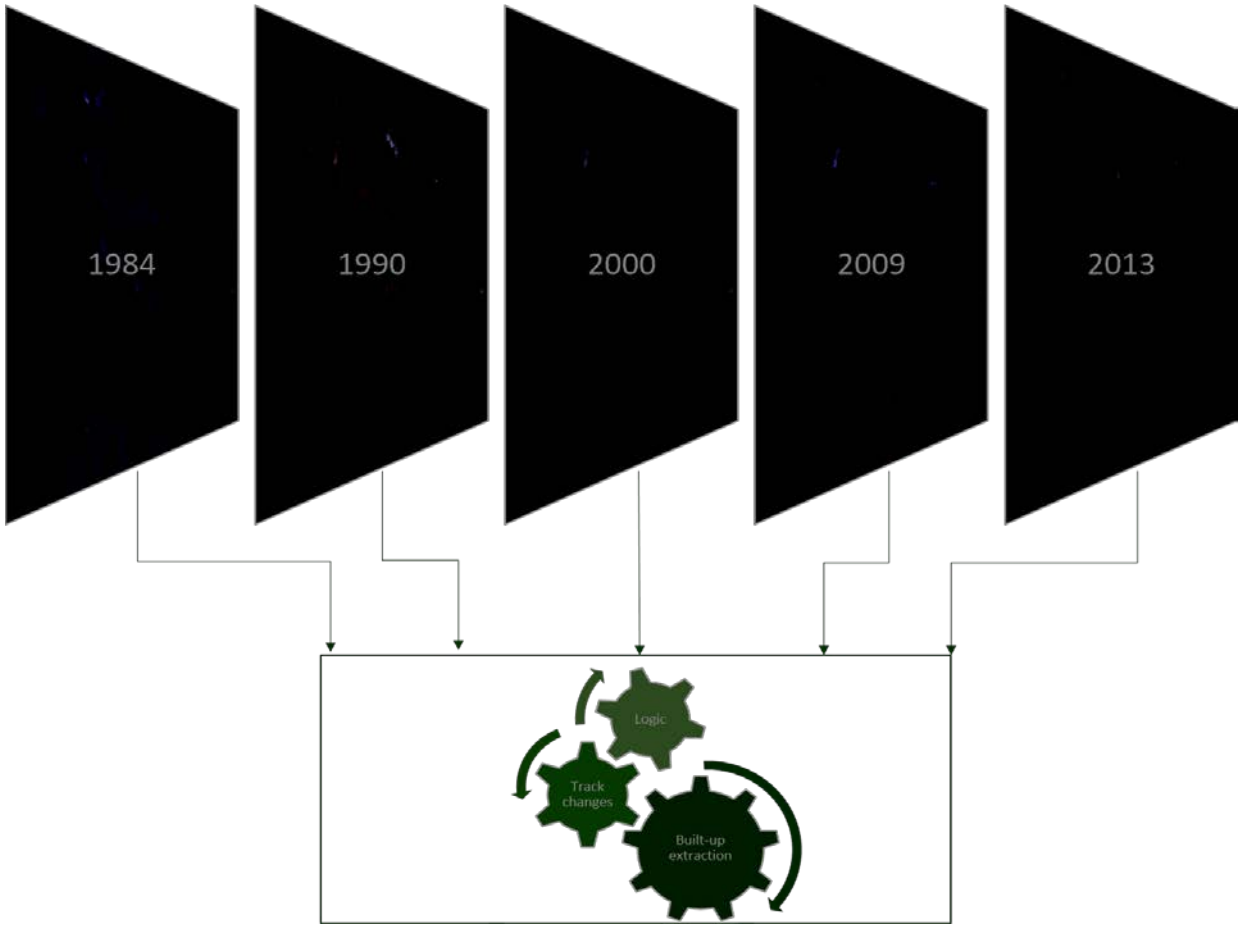

Figure 8: Change detection conceptual scheme.

4. Supervised methods

The input of the post-classification filters can be produced using a supervised classification

approach. The end-users can easily define training sets and apply them to the Landsat imagery. Results can be used as input for the post-classification filters. With respect to the unsupervised approach, this method is less automatized and more user-skills-dependent.

5. Improvements by filtering

Different filters based on the continuity among the extractions year after year have been developed. The main goal of these filters is to try to improve the initial results and to fix the errors introduced by the different built-up extraction methods.

Single changes filter

The scope of this filter is to recognize the segments with a “stable” behaviour through the years. The “stable” label is associated with segments with a continuous behaviour; an example is provided with Figure 9 where the segment follows the expected growth in time of a built-up area. Figure 9. Such a change occurring to the segment state would probably be due to the expansion of the built-up area.

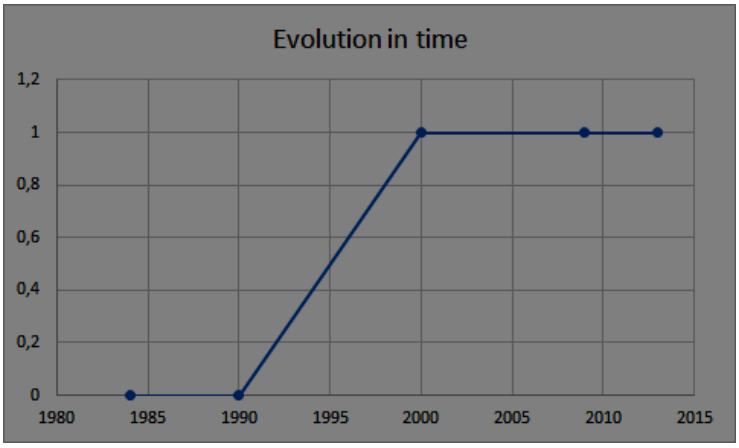
Evolution in time
1,2
1
0,8
0,6
0,4
0,2
0
1980
1985
1990
1995
2000
2005
2010
2015

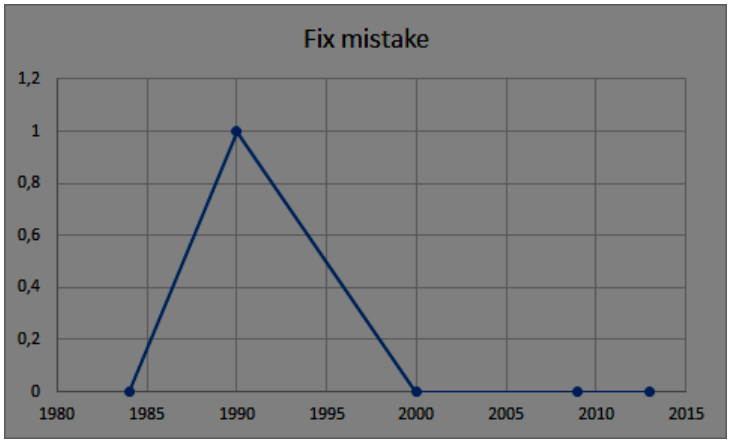

Figure 10: Example of how the method can fix the unstable results. The segment shows an unstable behaviour that can be interpreted as a misclassification from year 1990 and consequently corrected

Double changes filter

Every segment that is not classified as stable from the first filter is further processed taking into account the continuity over time. The main idea is to consider a window 4-observations long and evaluate changes in time; continuity is the metric used to decide whether the segment was wrongly classified in one of the observations (see Figure 10).

Spatial filter

The third implemented filter takes care of the segments labelled as uncertain after the second filter (objects showing more than two changes). Segments around the undetermined segment are analysed and a decision is made according to the presence or not of stable segments around the one of interest.

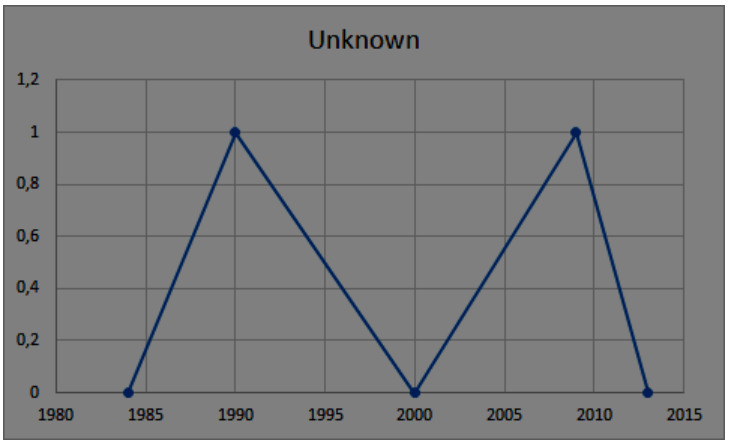

Figure 11: Example of case where the spatial filter will be applied because it is difficult to determine a precise pattern.

Unsupervised Temporal Analysis for Medium Resolution Images

6. Introduction

Remote sensing could play an important and effective role in the assessment and monitoring of change dynamics. While remote-sensing data analysis does not replace field inventory, it provides supplementary information quickly and efficiently. The use of remotely sensed data offers many advantages, including synoptic coverage, availability of low-cost or free satellite data, availability of historical satellite data, and repeated coverage. In addition, recent advances in the hardware and software used for processing a large volume of satellite data has helped increase the usefulness of remotely sensed data.

For many years, impervious surface mapping has produced records of urban maps that have been used to monitor disasters. The monitoring of changes in impervious surfaces, primarily associated with the rooftops of buildings and human transportation (streets and highways), using remote sensing technology is an important factor in disaster mapping and recovery monitoring. Imperviousness is one of the few variables that can be explicitly used to quantify and measure the impacts primarily associated with humans. Therefore, the accurate and quick estimation of impervious surfaces is critical for disaster management decision-making, monitoring and planning. Remote-sensing technology and geographic information systems (GISs) have greatly facilitated the monitoring of impervious surfaces and their changes. Several factors, such as image quality, data analysis methodology, interpretation techniques and numerous temporal considerations, significantly influence the quality of the resulting geospatial information (Vogelmann et al., 2001). Satellite remote sensing images have been applied for impervious surface estimation due to their relatively low cost and suitability for large area mapping (Bauer et al., 2004).

Methods used in classifying impervious surfaces

In the field of remote sensing, significant efforts have been placed in improving impervious surface classification accuracy. Different approaches have been applied, including the incorporation of geographic data (Harris & Ventura, 1995), census data (Mesev, 1998), texture features (Lu & Weng, 2005; Mint, 2001; Shaba & Daksha, 2001), and structure or contextual information (Gong & Howarth, 1990; Stockers et al., 2000) into remote sensing spectral data. Moreover, expert systems (Hung & Ridd, 2002; Stefanov et al., 2001), fuzzy classification (Zhang & Foody, 2001), and merged multisensor data such as those between radar and Thematic Mapper (TM) data (Haack et al., 2002), and between SPOT and TM data (Gluch, 2002) have been applied. Much attention has recently been shifted to the development of more advanced classification algorithms (Green et al. 1994, Wolter et al. 1995, Kaufman and Seto 2001), including neural networks and contextual, object-oriented, and knowledge-based classification approaches (Stuckens et al., 2000; Thomas et al., 2003; Zhang & Foody, 2001; Zhang & Wang, 2003).

Issues with traditional classification methods for medium resolution images

The analysis of impervious surfaces is fundamentally different from many other applications of optical remote sensing. Traditional hard classification methods, such as Maximum Likelihood classification, have generally been effective in the urban environment (Green et al. 1994, Wolter et al. 1995, Kaufman and Seto 2001). But they are predicated on the assumption that landcover classes are spectrally distinct at pixel scales and therefore occupy separate regions of the spectral feature space. The characteristic spatial scale of urban landcover is comparable to the size of the pixel of the most widely used operational multispectral sensors (e.g., Landsat TM, Multispectral Scanner, SPOT) (Small, 2001b; Welch, 1982). This results in a large percentage of ‘‘mixed pixels’’ for which the observed radiance is a mixture of distinct radiances from features with different reflectances within the large GIF pixel size. Mixed pixels violate the cardinal assumption of hard classification methods, but, in some cases, they may be characterized by simple combinations of target materials contributing to the observed radiance. Post-classification comparison first classifies multi-temporal satellite images into land-cover classes independently at each date and then compares the classified land-cover sequences successively over time to construct the trajectories of land-cover change.

Issues with post-classification methods used in change detection

To date, post-classification comparison has been used predominantly for reconstructing land-cover change trajectories in various land use and landcover change studies (Lucas et al. 1993). It is well known, however, that the accuracy of post-classification comparison is highly dependent on the impervious classification results at each date. Landcover classification from satellite imagery inherently possesses various classification errors caused by factors such as noise in satellite observations, spectral confusion among different land-cover classes, and limitations of classification algorithms. Consequently, when multi-temporal land-cover results of the same area are combined, classification errors generated at each date will inevitably be propagated to the post-classification comparison process, potentially leading to poor accuracy in the resulting change trajectories (Singh, 1989). The change map product of two classifications often exhibits accuracies similar to the product of multiplying the accuracies of each individual classification (Stow, 1995). This issue becomes increasingly more critical as more time steps are involved in post-classification comparisons. Therefore, to achieve sufficient accuracy on land-cover change trajectories, accurate and consistent land-cover classification results across space and time are needed for multi-temporal post-classification comparisons. To this end, spectral information directly from satellite observations is usually not enough, and the spatial and temporal context related to land-cover change trajectories must be incorporated into the classification (Boucher et al., 2006).

7. Proposed method: Trajectory-based change detection

Recently, trajectory-based change detection techniques have been developed to study land cover change (Main-Knorn, et al., 2013). This technique was initially developed to detect land-cover transitions between two dates (i.e., “from–to” land-cover changes), and its extension to more than two dates represents a natural way to track land-cover change trajectories over multiple dates. Trajectories are defined as the trends among the relationship over time between the factors shaping the changing nature of the environment and their effects within a particular region. A land-cover change trajectory refers to the successive areas of land cover types in a time series. The reflectance of impervious urban areas vary less over time compared to other land cover types (Liu et at. 2014). In trajectory analysis, the impervious urban areas determined from urban indices change relatively less compared to the surrounding vegetation. The variations in vegetation over time are captured and segmented to a class that captures the change in the vegetation greenness. The modest or non-existent change can be statistically captured and segmented into a separate class using trajectory-based change detection. Similarly, suburban areas mostly dominated by vegetation are captured and segmented as a different class.

Preparation of data for trajectory-based change detection

The detection of change over time of land-cover from spectral signatures, despite its wide use, is affected to various degrees by the following factors: temporal changes in shading due to topography and sun angle, distortion caused by differences in viewing angles in temporal images, inaccuracies in georeferencing, and atmospheric scattering and absorption of light. Atmospheric correction of the radiation received at the satellite is by far the most difficult correction to make. Electromagnetic radiation collected by satellites is modified by scattering and absorption by gasses, water vapor, and particulate aerosols. A number of radiative transfer models based on ray tracing algorithms have been developed for correcting the atmospheric effects. Singh, 1989 has shown that these models can accurately correct for the atmosphere. However, these corrections require accurate measurements of atmospheric optical properties. These measurements are often not available or are not exactly in the study area or coincident with the overpass. Since more light scatters at shorter wavelengths, the blue band is more sensitive to atmospheric effects than the red and infrared bands commonly used for vegetation indices. Thus, unless one uses data that

have been atmospherically corrected, the use of the blue band is less desirable than methods that use only the red and infrared bands.

Before a time series of remotely sensed imagery can be used in a change detection study, the images must first be standardized for conditions outside of real surface change. Differences in the sensor, solar illumination or atmospheric conditions make it difficult, if not impossible, to accurately compare satellite images acquired on different dates. Normalizing bands help to correct for atmosphere changes. Adjusting imagery for atmospheric attenuation reduces the variation between temporally separate images so they appear to have been acquired under the same solar and atmospheric conditions, allowing for the more accurate detection of landscape change. As a result, it is widely recognized that a set of remotely sensed images must be radiometrically normalized before being used in a change detection study. There are a number of normalized indexes that have been developed over the years primarily for the purpose of ecological assessment, although not directly for determining land use. The NDVI is the most commonly used index for ecological assessment (Elmore et al., 2000). Indices for mapping the built-up and bare land in urban areas, such as the Normalised Difference Built-Up Index (NDBI) (Xu, 2007), Index-based Built-Up Index (IBI), EBBI (Enhanced Built-up and Bareness Index), Urban Index (UI) (As-syakur A. R.et al 2012), Normalised Difference Bareness Index (NDBaI) (Li, et at., 2014), and Bare soil index (BI), have been employed in various studies. Inaddition to the above indices LSWI (Land Surface Water Index), NBR (Normalized Burn Ratio), NDSI (Normalized Difference Snow Index), NDWI (Normalized Difference Water Index) 1, (Chen, et. al 2006), NDWI 2, NDWI3, CTVI (Corrected Transformed Vegetation Index), Thiam's Transformed Vegetation *Index* (*TTVI*) were used in this study.

The examination of a temporal sequence of satellite images allows changes in the reflectance associated with disturbance to be quantified and can be used to characterise disturbance events such as disasters effectively. The key advantage of analysing multiple images, rather than a single image, is that a record of spectral reflectance change can be extracted to characterize both the magnitude and direction of physiological processes or disturbance events rather than seeking only the contrast between features of a single date of imagery.

Statistical clustering

Statistical clustering of the trajectories involves clustering the pixels of an image into a set of classes, such that the pixels in the same class have statistically similar trajectories. The clustering depends on distinctive properties of the trajectory. In an unsupervised clustering method, the user specifies the number of clusters into which the pixels need to be clustered. There are numerous clustering algorithms (Duda and Hart, 1973) that can be used to determine the natural spectral groupings present in a data set. One common form of clustering, called the “k-means” approach, requires the number of clusters to be located in the data by the analyst. The algorithm then arbitrarily “seeds” or locates that number of clusters’ centers in the multi-dimensional measurement space. Each pixel in the image is then assigned to the cluster whose arbitrary mean trajectory is closest. The basic premise is that trajectories within a given cluster type should be close together in the measurement space, whereas trajectories in different classes should be comparatively well-separated. The pixel trajectory around the mean trajectory depends on the temporal variability of the pixel and the area extent of the land type variations over time.

Data

Landsat’s free web-based access has greatly improved the accessibility of multi-temporal Landsat

data (USGS 2008), opening up an unprecedented opportunity to advance land-cover change trajectory analysis for LULCC studies. Landsat ETM satellite images have 8 bands, including a thermal and a panchromatic band. Landsat OLI satellite images have 10 bands, including a thermal and a panchromatic band. In visible, near infrared and middle infrared regions, Landsat images have a 30 m spatial resolution. However, in thermal and panchromatic regions, spatial resolutions are 60 m and 15 m, respectively. With 16 days of temporal resolution, Landsat ETM+ was the ideal satellite image for change trajectory analysis.

Date	Sensor
2007-07-24	Landsat 5/ETM
2007-09-10	Landsat 5/ETM
2009-07-13	Landsat 5/ETM
2010-06-14	Landsat 5/ETM
2010-06-30	Landsat 5/ETM
2010-08-01	Landsat 5/ETM
2010-08-17	Landsat 5/ETM
2011-06-07	Landsat 5/ETM
2011-07-03	Landsat 5/ETM
2013-06-06	Landsat 8/OLI
2013-07-08	Landsat 8/OLI
2013-07-24	Landsat 8/OLI
2013-08-25	Landsat 8/OLI
2013-09-26	Landsat 8/OLI
2013-10-12	Landsat 8/OLI

Table 1: Series of Landsat ETM (2007 -2011) and OLI (2013) images of Van, Turkey.

Output

The predefined normalized indices are derived for each date and stacked to create an image cube. Then, the data are statistically clustered into 20 clusters or classes. based on their temporal variability. The vegetation indices vary in proportion to the ratio of infrared and red reflected energy. Hence the vegetation Indices vary proportionally to the vegetation content over time. Similarly, the building indices are a good indicator of the impervious surfaces. The spatial distributions of the classes are shown in figure 12. Figures 12 and 13 show the temporal variability of the means of the 20 clusters of pixels or classes for vegetation and a built-up area index.

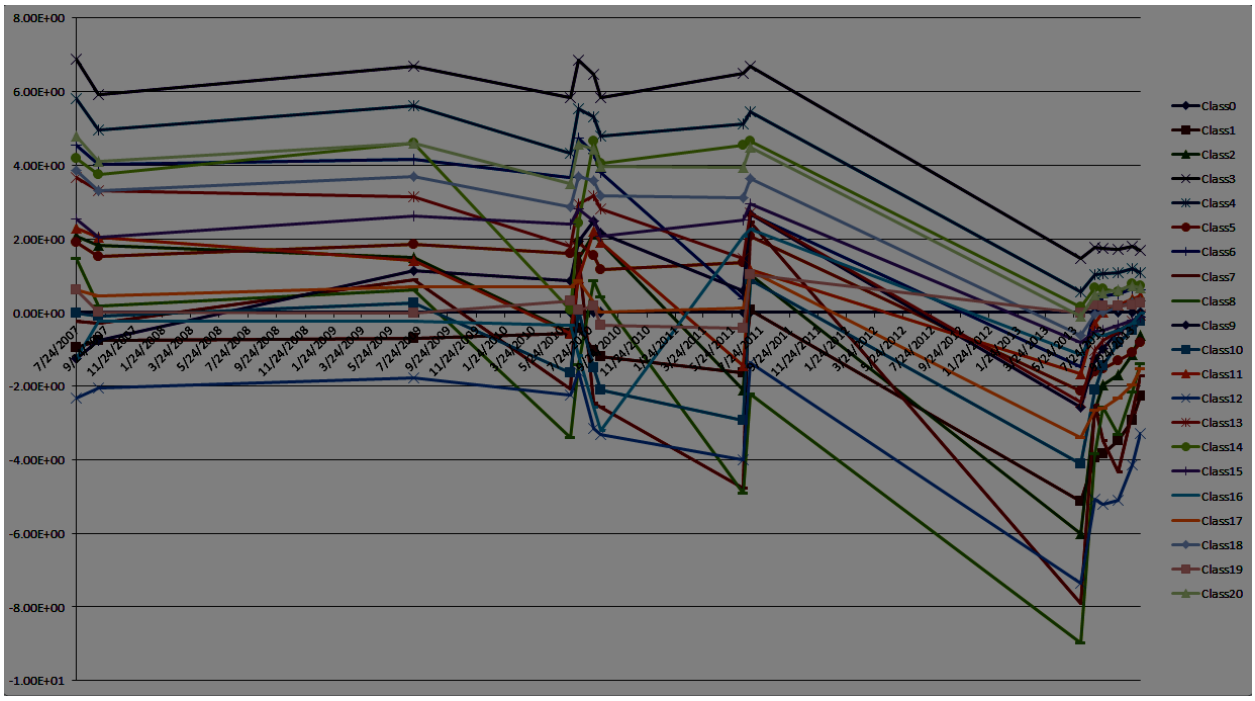

Figure 12 The trajectory means of the Enhanced Built-up and Bareness Index (EBBI) of twenty clusters or classes. Based on the shape and the properties of the trajectory, the classes can be identified as areas with varying impervious area percentages.

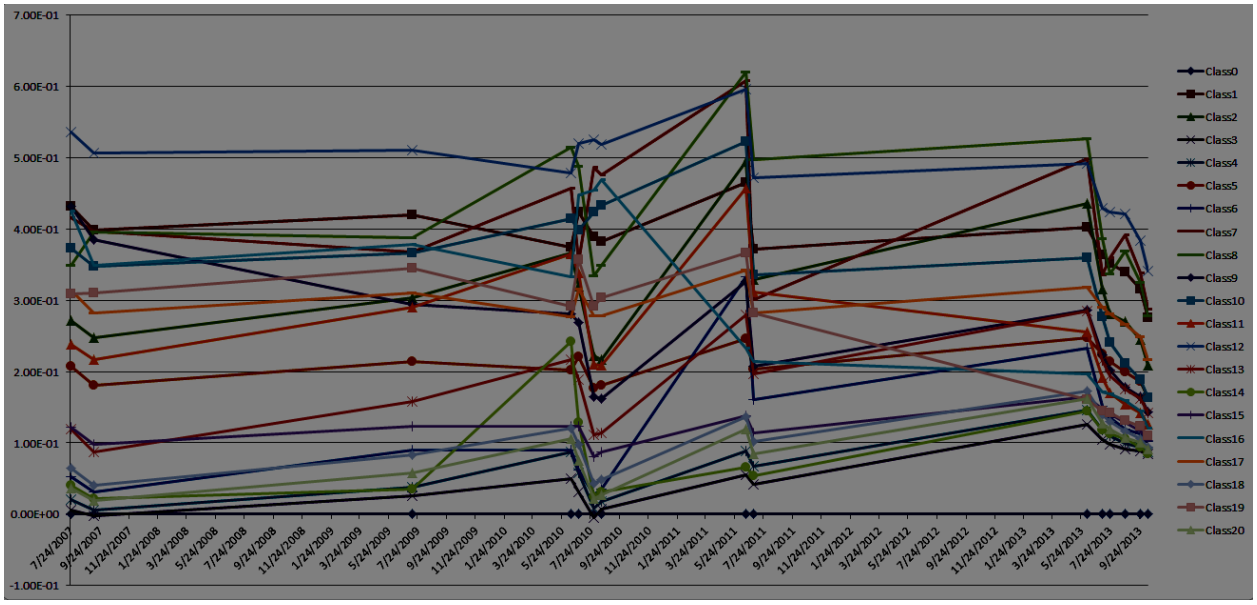

Figure 13 The trajectory means of the Normalized Difference Vegetation Index (NDVI) of twenty clusters or classes. Based on the shape and the properties of the trajectory, the classes can be identified as areas with varying greeness area percentages.

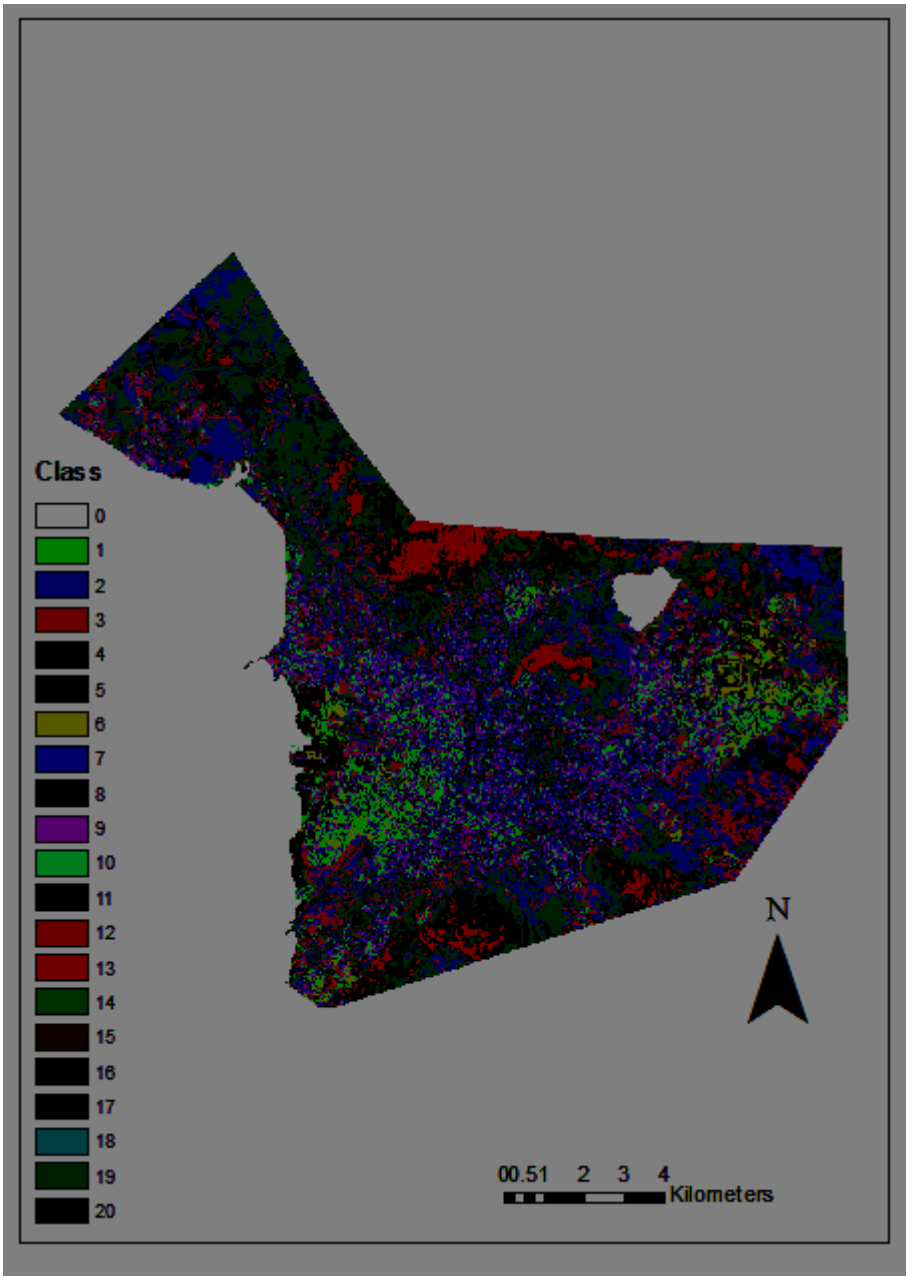

Figure 14 Medium resolution classification done using the SENSUM automated trajectory-based method for Van, Turkey. Shown are 20 classes based on the temporal trajectories of pixels.

Relative change between dates

Next we look at changes in the Vegetation Index and the Built-up Index. We see that in some classes, there are sharp increases and decreases in vegetation and built-up areas over time, represented by the gradient of the temporal trajectory. For this purpose, we look at the gradient changes between dates of images. The rate of change which is the gradient is plotted to see the change visually (Figure 13).

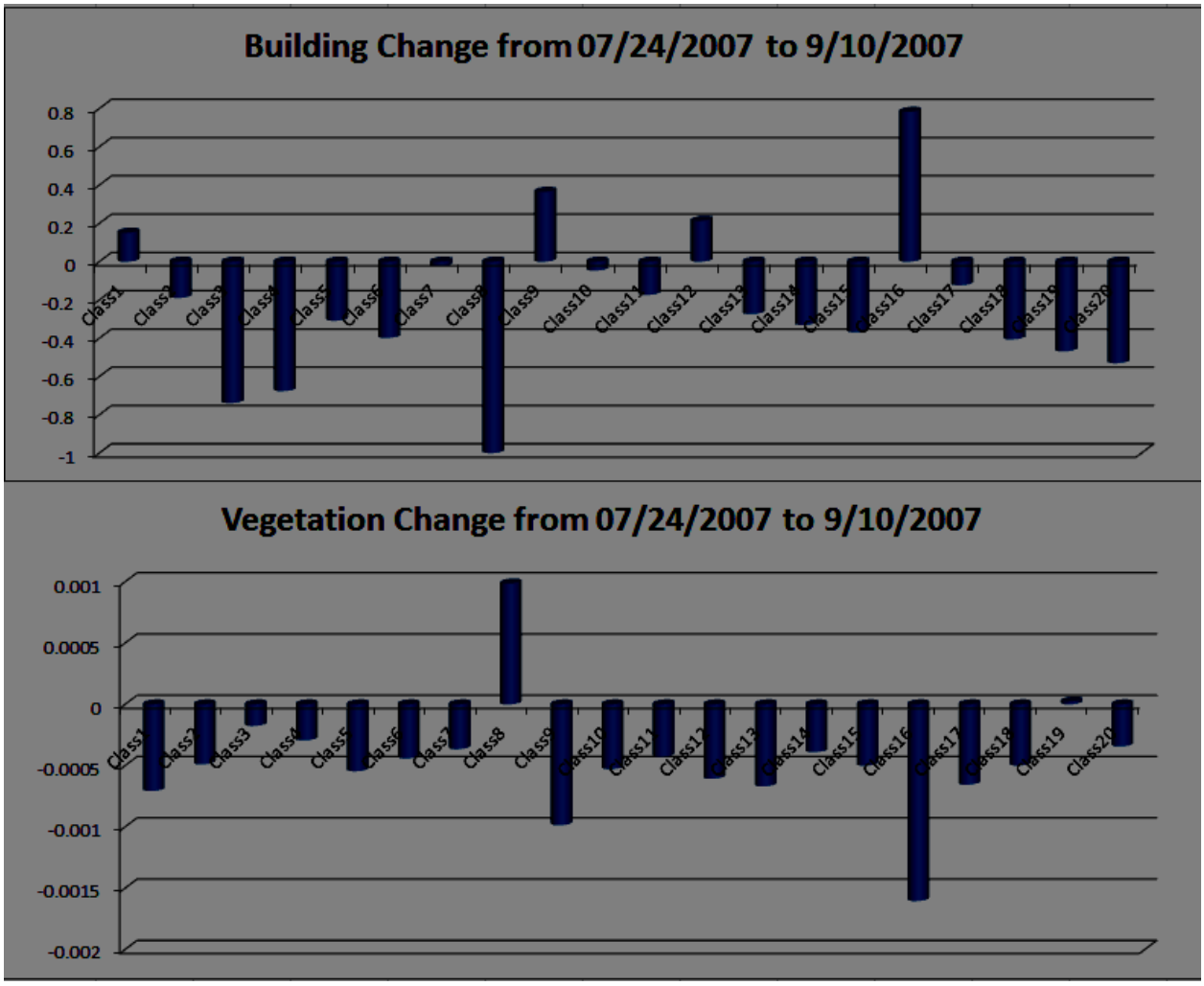

Figure 15 The rate of change (gradient of the trajectories) between the dates 07/34/2007 and 9/10/2007. The vegetation index is used to determine the amount of vegetation in each pixel. The vegetation Index used here is the NDVI and the building Index used above is EBBI. There is an overall decrease in vegetation in all the classes.

From Figure 15, it is clear that class 16 has decreased in vegetation and increased in built-up area most, relative to the other areas. Class 8 shows the opposite effect, with increased vegetation and decreased built-up areas. Class 3 and 4 show a decrease in built up area without much increase in vegetation. The classes are in turn plotted on a map as shown in the figure below (Figure 16).

a)	b)

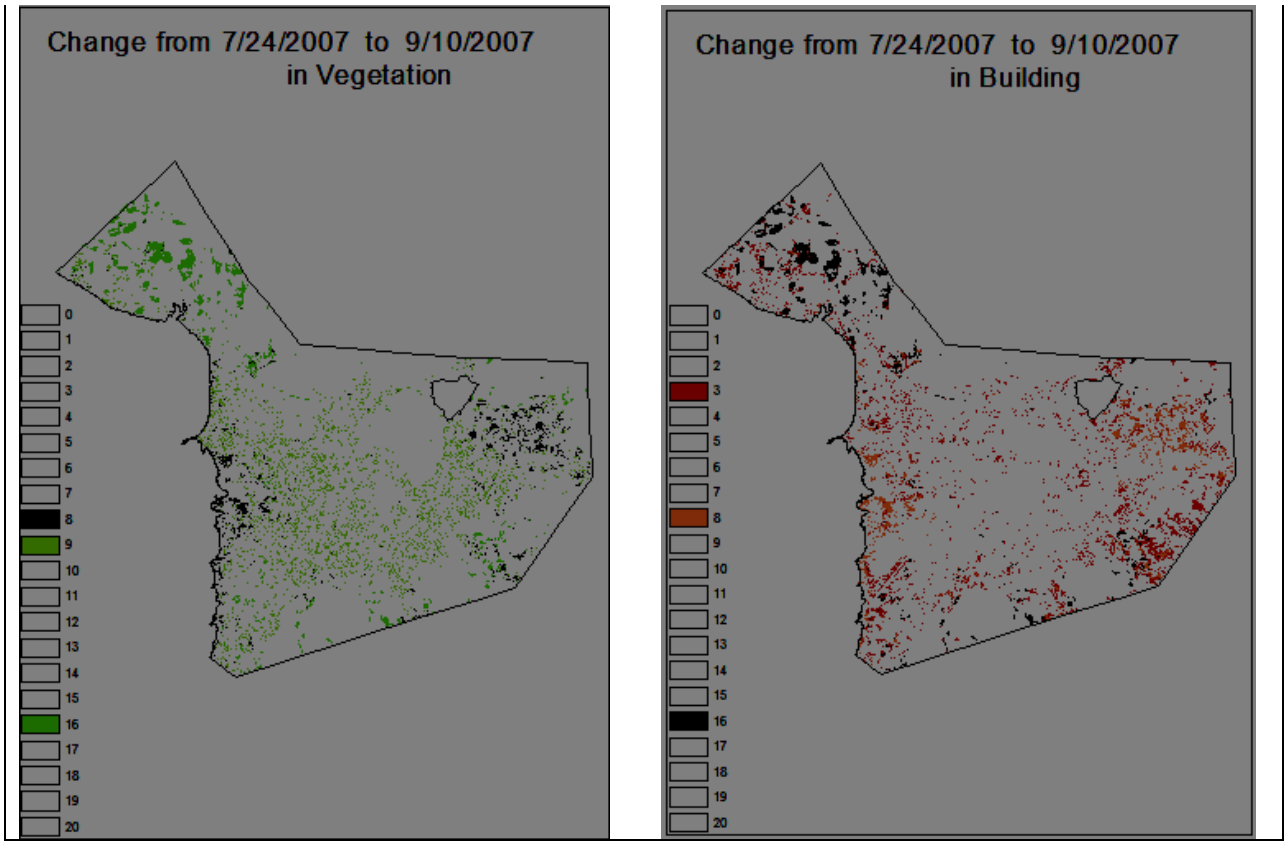

Figure 16 a) Shown in Dark green are the areas that vegetation has increased and shown in light green is areas the vegetation has decreased compared to other areas. b) Shown in Dark brown are the areas that built-up areas has increased and shown in light green is areas the built-up areas have decreased compared to other areas.

Next, we look at the difference between another two dates, namely 09/10/2007 and 7/13/2009.

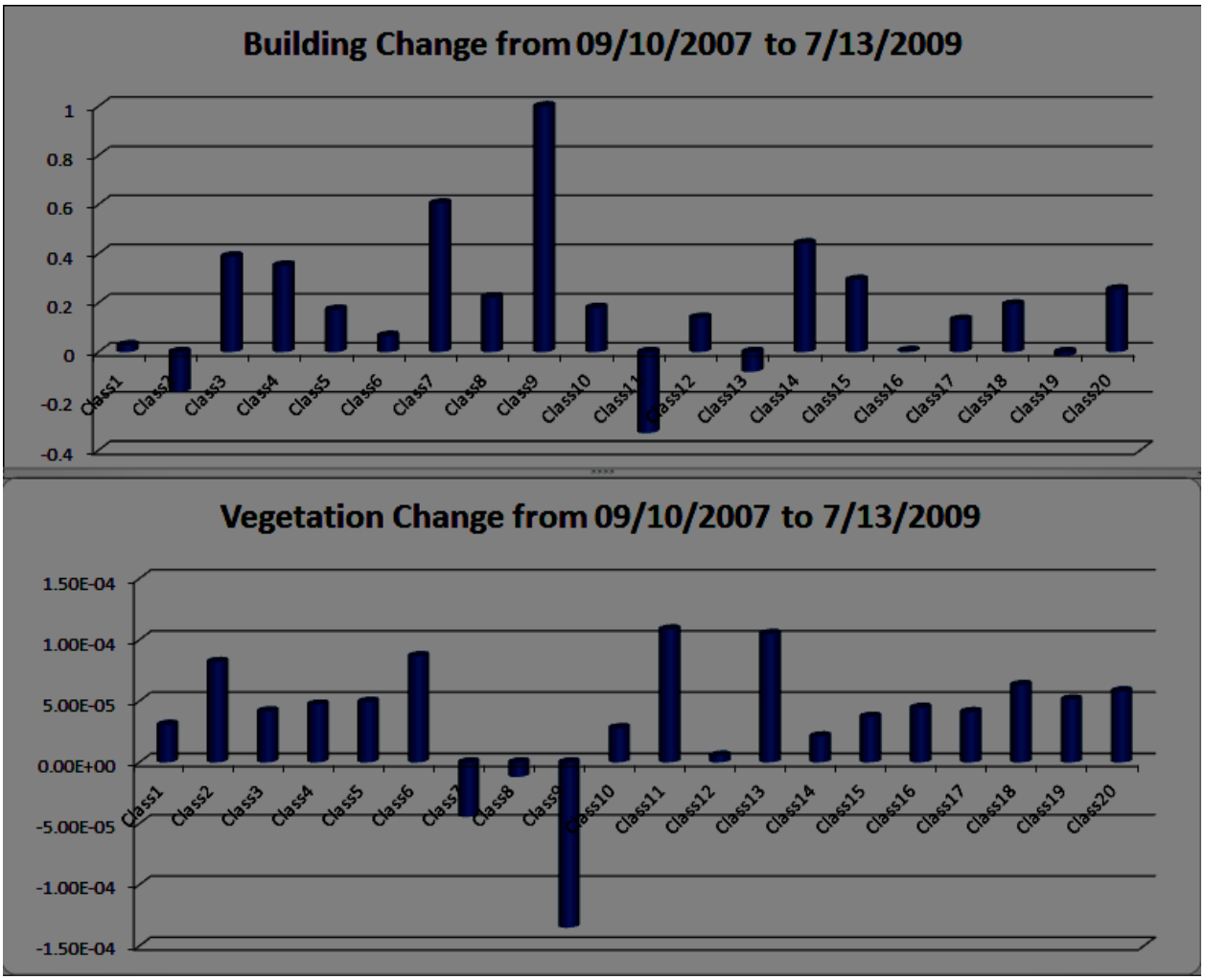

Figure 17 The above show the rate of change (gradient of the trajectories) between the dates 09/10/2007 and 7/13/2009. There is an overall increase in vegetation in all the classes except the relative decrease in class 9.

From the above figure, it is clear that class 9 has decreased in vegetation and the area has increased in built-up area relative to the other areas. Class 7 has increased in built up area while having very little decrease in vegetation.
The increase and decrease in the classes are plotted on a map as shown in the figure below.

a) b)

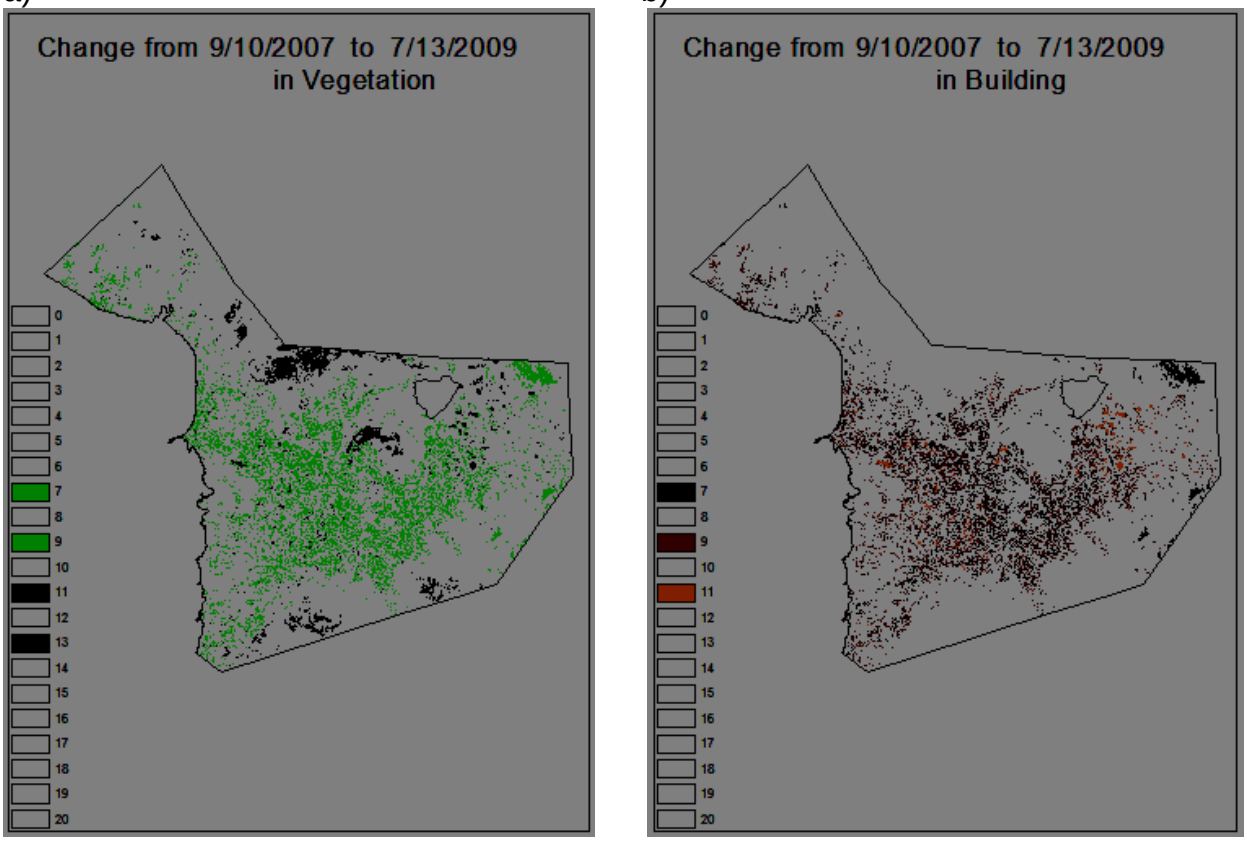

Figure 18 a) Shown in dark green are the regions where vegetation has increased; shown in light green are areas the vegetation has decreased compared to other areas. b) Shown in dark brown are the regions where built-up areas have increased; shown in light green areas regions where the built-up areas have decreased compared to other areas.

Discussion

In this section, an automated method that can be used on moderate resolution images for identifying areas of change over time is discussed. The method proposed would map the aerial changes to built-up areas relative to the vegetation. One application of this method could be to look at new developments. Such a view could be also used to calculate the building age and thereby use the data in building vulnerability assessments based on the age of the buildings. The age of buildings and the time of construction could then be used as proxies for the vulnerability of buildings to earthquakes, for example, due to building code issuance and implementation of that time. This method can also be used and will be tested in deliverable D5.3 “Case studies on data-rich and data-poor countries” as a focal mapping technique. Moderate resolution images are free and readily accessible. High resolution images are costly and in order to minimise time and cost, this temporal analysis technique can be used to reduce the areas of interest for high resolution analyses. The high resolution change detection techniques reviewed for SENSUM will be presented in the next section. Some of these techniques, as will be shown in Deliverable 5.3, will make use of unsupervised temporal analysis of medium resolution images to help constrain the examined images.

Unsupervised Object Based Change Index for High Resolution Images

8. Assessment of change in complex environments

For the SENSUM project, the review and use of change detection techniques for high-resolution images has been for post-disaster recovery monitoring. Following a disaster, change detection is a prerequisite for the assessment of progress in relief and recovery.
The key to monitoring recovery is measuring incremental change; it begins with the base state and the initial impact due to the event. That initial change, besides measuring the impact, is also (when used comparatively) a measure of robustness, which can be evaluated based on the rate of recovery. The figure below shows a sequence of what can be seen from high-resolution remotely sensed images in terms of changes to building progress over time. This set of images are of a fishing village in Thailand following the Boxing Day Tsunami of 2004.

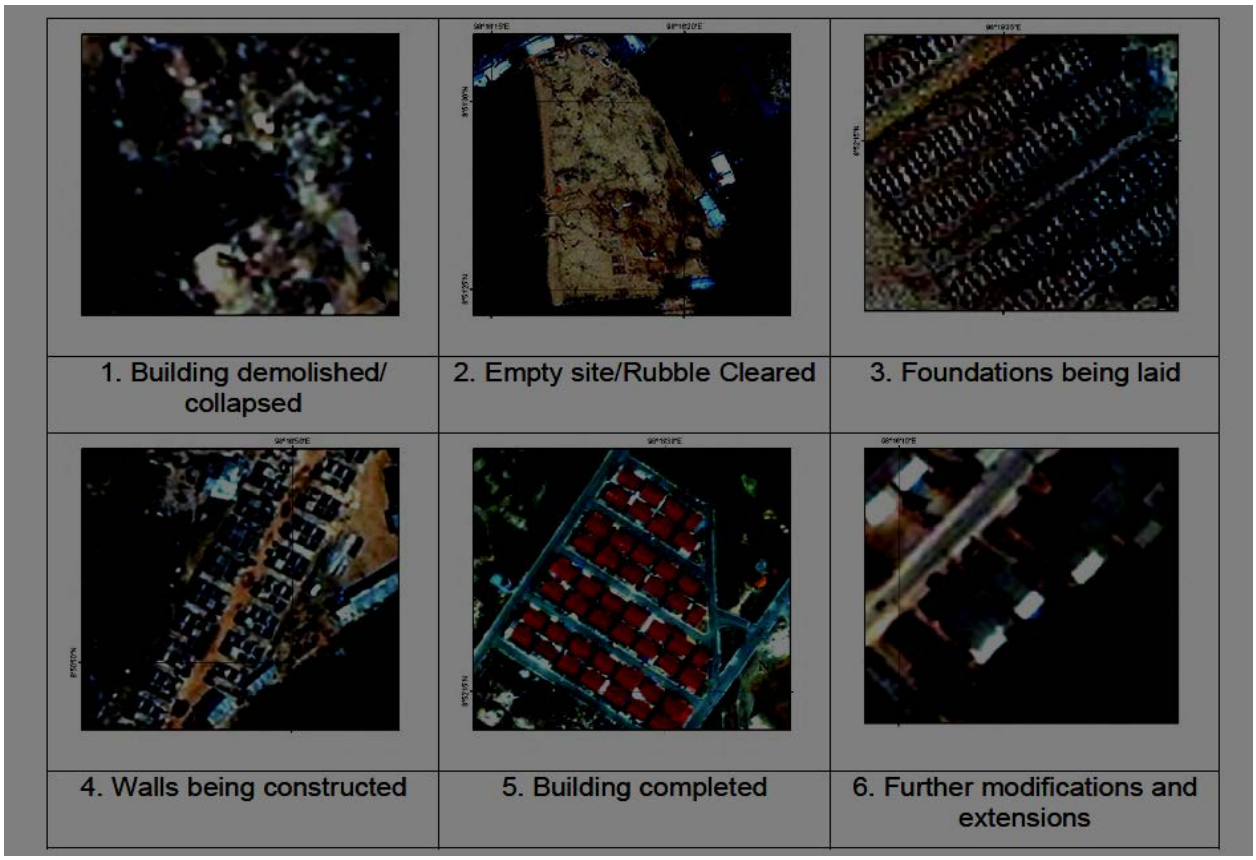

Figure 19 A sequence of high resolution images showing the recovery of a development from the base state of total destruction to new buildings and modifications to buildings, signifying the growth and recovery of the affected community.

Many algorithms have been developed, but very few have been applied to urban studies to update maps from high spatial-resolution remote sensing images. Remote sensing satellites equipped with Very High Resolution (VHR) optical sensors can provide important information about the affected areas since they can map the regions of interest quickly, with a high geometric precision (Walter,

2005). The semantic richness of more resolved images increases, while making image analysis more difficult. Change detection from high spatial resolution images such as IKONOS and QuickBird is even more challenging, especially in complex environments like urban areas characterised by small objects (such as houses, individual trees, and roads) and by shadows. Information on the changes to the building fabric caused by an event can be derived from suitable satellite imagery by comparing data from a chosen reference before the event (pre-event) to imagery acquired shortly after the event (post-event). Optical (VHR sensors (*e.g*., QuickBird) have the appropriate resolutions. Some of them have existed for almost a decade and have already imaged large parts of the Earth. The increased availability of such sensors and their growing, frequently updated image archives make VHR optical data well suited to be the pre-event and post-event reference data source. The availability of pre- and post-event data opens the possibility for gathering impact assessment data using change detection.

9. High resolution change detection techniques

In general, change detection techniques can be grouped into two types: Pixel-based and Object-based. Pixel-based change detection analysis refers to using change detection algorithms to compare the multi-temporal images pixel by pixel, while object-based change detection analysis refers to using change detection algorithms to compare the multi-temporal images object by object. However, the definition of pixel-based and object-based change detection is not distinct.

Pixel-based method

There have been many pixel-based change detection algorithms proposed, such as image differencing and image ratio-ing, which can only provide change/non-change information. These techniques are easy to implement, but the threshold, which is the key to get good change detection results, is difficult to determine. It is simple and straightforward to interpret the results, but they cannot provide details of the change and require the selection of thresholds. One of the limitations of traditional pixel-based change detection approaches is the difficulty to model the contextual information for every pixel by the moving window with the size and shape particular to the corresponding object. However, most impact assessments to date have focused on the detection of man-made objects such as buildings, roads, bridges, *etc*. Although object based methods give much better results than the traditional pixel-based techniques, analysis for choosing optimized object features is not straightforward. This is a very complex task because the high information content of VHR images requires an accurate definition and modelling of the concept of an object (which is often associated with the specific goal of the application) and thus the development of techniques should take into account the accuracy needed for the application.

Object based method

The most basic feature of the object-based approach is to segment the image and regard the objects as the basic unit of operation, rather than the pixel-based approach which regards a single pixel as the basic unit of operation (Dai, et al., 1998). For detecting the objects, most methods deal with rectangular building detection, which is complex and of a low accuracy, especially after disasters. Building damage from disasters gives rise to irregular patterns, making object detection based on pattern recognition very difficult.

Although object segmentation is not new, only a few of the existing approaches lead to qualitatively

convincing results while being robust and operational. Choosing objects in change detection is the step with the largest error in object based change detection methodologies. The advent of high-spatial-resolution remote-sensing imagery further provides opportunities to obtain GIS data of man-made objects that facilitate shelter and accessibility prior to disasters. Hence, using GIS objects pertaining to indicators (building footprints, open spaces, roads, bridges, *etc*.) derived from the WP2 algorithms as the pre-disaster GIS objects and targeting the search for specific changes to the areas within the objects can increase the accuracy in the change detection process.

10. Proposed method: GIS object based method

To increase the accuracy of detecting buildings with varying degrees of change, we propose an object-based change detection method. Typically for change assessment for recovery management, the users need an automated and robust method. Hence, indicators such as building footprints, open spaces, roads, bridges, *etc*., derived from the WP2 algorithms, or existing GIS maps, can be used as the GIS objects. The subsequent specific change within the areas of the objects can be studied more accurately. By looking at these objects in pre- and post-disaster images, we can better identify indicator-specific differences and thereby increase the accuracy in the change detection process.

This indicator-specific method uses readily available pre-disaster GIS data and integrates existing knowledge into the processing flow to optimize the change detection while offering the possibility to target specific types of changes to man-made objects. The indicator-specific information of the GIS objects is used as a series of masks to treat the GIS objects with similar characteristics in an equivalent manner for better accuracy. The above proposed approach is based on a fusion of a multi-index change detection methods based on gradient, texture and edge similarity filters. The change detection index is flexible for disaster cases in which the pre-disaster and post-disaster images are not of the same resolution. The proposed automated method is evaluated with QuickBird and Ikonos datasets for abrupt changes soon after a disaster. The method could also be extended to a semi-automated way for monitoring progressive changes in the months following the disaster.

11. Description of the Method

Once we identify the urban areas from the temporal analysis of medium resolution images (as explained in the previous section), we can then work with high resolution data within the urban areas. Changes within the indicator-specific GIS objects are used for better accuracy in the change detection process. The indicator-specific objects are roads, bridges and the like, buildings, open areas, and other infrastructure. Based on the changes within the indicator-specific GIS objects, indices are calculated and plotted over time.
For the object based change index, the indicator-specific GIS objects are used as a series of masks to determine the changes within the GIS objects. The index is built based on the following for each of the GIS objects. For each indicator-specific GIS object, the following is calculated based on the pre- and post-images. Change is identified as the absence of similarity.

- ***Similarity of gradient.*** In order to rule out changes caused by such atmospheric and illumination factors such as radiance intensity and colour changes.
- ***Similarity of texture***. In order to better gauge whether the roof structure of the object has changed over time.
- ***Similarity of edges.*** In order to see the changes of the edges which could be a

good estimate of the condition of the structure of the object.

All of the above were used on the pre- and post-images separately, on a fused image consisting of the pre- and post-images (Figure 21). Hence, the indices reflect the changes in the gradient, texture and edge changes.

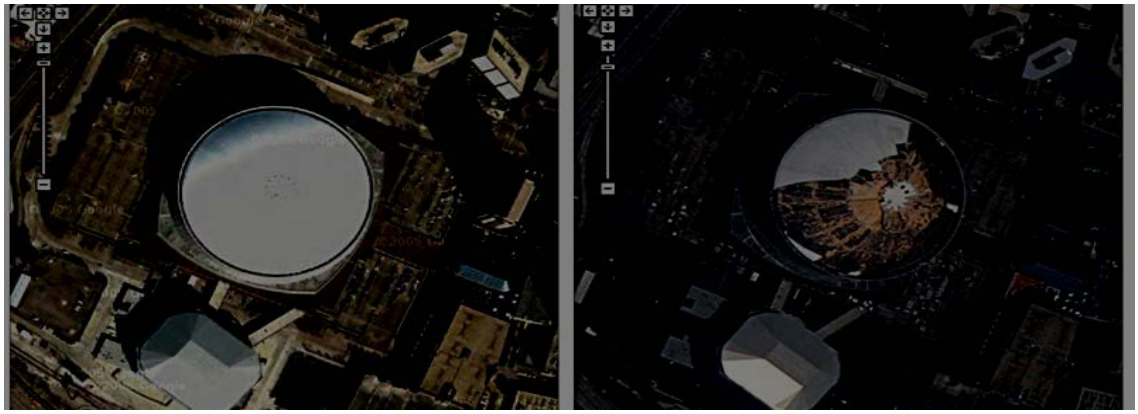

Figure 20 Pre and post images of town hall in New Orleans before and after the Hurricane Katrina show the textural and edge differences. The gradient function takes in to account the illumination differences. Images from google Maps (Google 2005)

Method

A) The pre and post images are fist PAN sharpened and then co-registered to the PAN image of the pre disaster image.

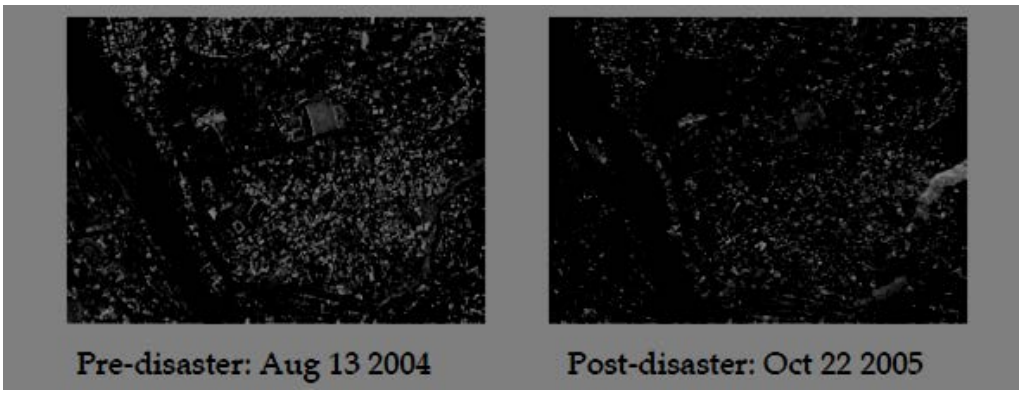

*Figure 21 The pre and post images of the **2005 Kashmir, Pakistan earthquake** occurred on the 8 October 2005. The above images are normalized to create a Normalized Change Detection Index (NCDI) using equation 1.*

$$= \frac{\left(\frac{Pre-Post}{Pre+Post}\right)\sqrt{ABS\left(\frac{Pre-Post}{Pre+Post}\right)}}{ABS\left(\frac{Pre-Post}{Pre+Post}\right)}$$ ——————— Equation 1

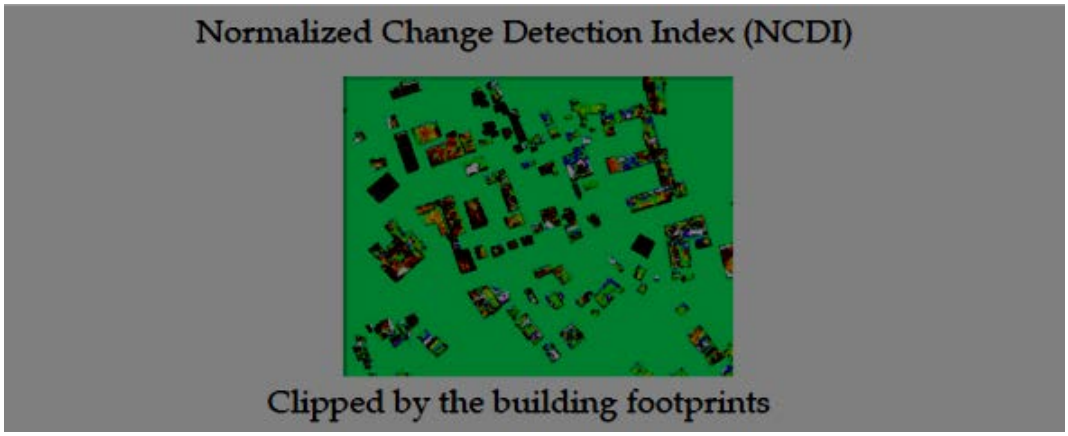

Figure 22 The pixel based NCDI calculated using equation 1

The normalized image is clipped by the object of interest. The objects shown above are building footprints. For each of the buildings, a Roughness coefficient calculated from QGIS' GDAL roughness function for the pixels within the building is calculated.

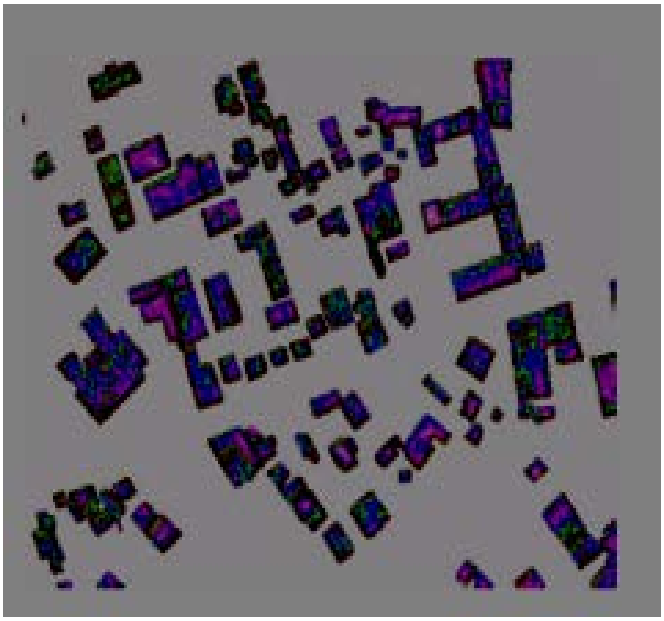

Figure 23 The pixel-based roughness parameters calculated from QGIS's GDAL Roughness parameters that are then averaged to obtain a single value for each building.

B) Next a 2 m buffer around the buildings is used to clip the edges of the buildings. The edges are then calculated and averaged for each building.

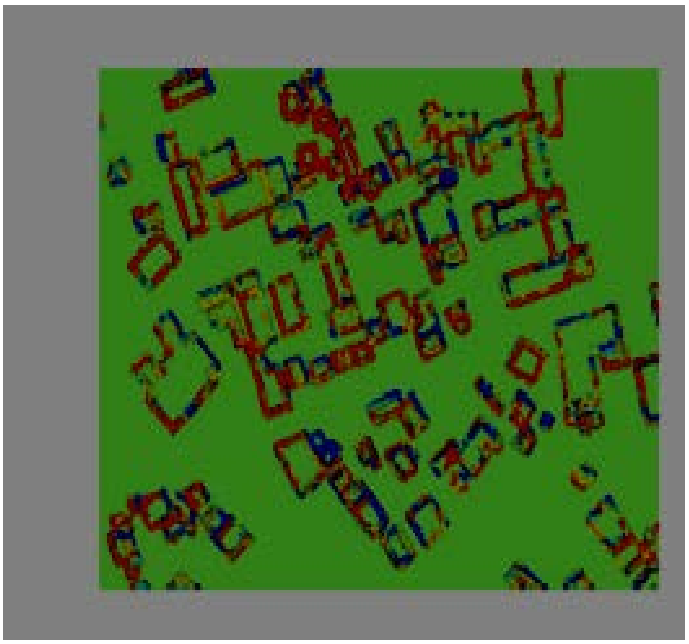

Figure 24 Shown above is the edge enhancement on the buffer of the buildings. The edges are calculated for the pre- and post-; then they are normalized using equation 1. Then the NCDI is averaged for each building.

C) Next for each building, the gradient is calculated for the original pre- and post-images.

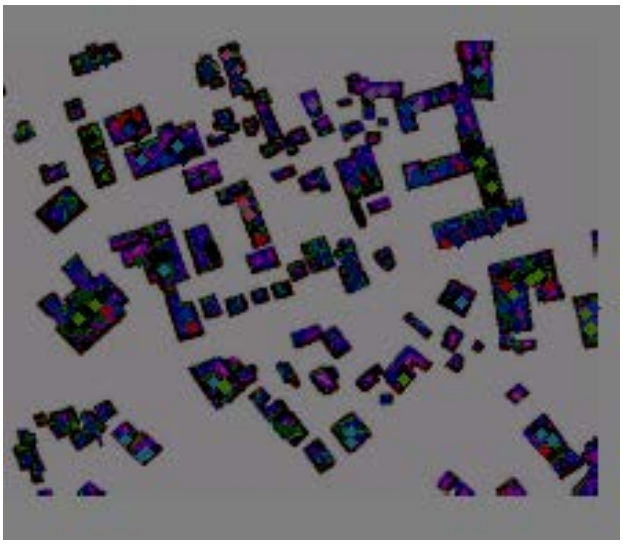

Figure 25 The pre- and post- images are then combined into a Normalized Index given by equation 1.

Once the Normalized index is calculated, the average value is calculated for each of the buildings.

The coefficients obtained from steps A), B) and C) are regressed against a visual index for each house. The combined index is called Enhanced Change Detection Index. Thereby every object will have a value pertaining to its change.

The Visual Index is obtained by looking at pre- and post-images of the buildings and giving each building a number between 1 and 10 based on the visual change. If the building is not changed relative to the other buildings, they are assigned a number close to 1. The buildings that are destroyed completely in the postimage are assigned a value close to 10.

Pre -disaster	Post - disaster	Visual Change Index
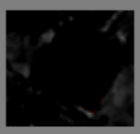	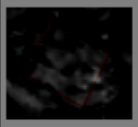	8
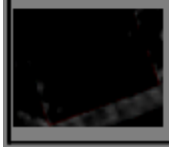		2

Pre - disaster	Post - disaster	Visual Change Index
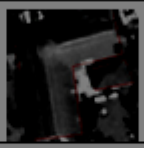	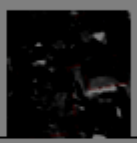	10
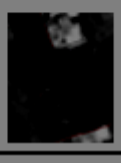	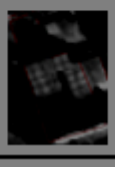	4

Figure 26 For the purpose of validation, a visual change index for a random set of 66 buildings were created based on the pre and post disaster images of ***2005 Kashmir, Pakistan earthquake****.*

Once the visual index is calculated, some random buildings are selected for validating, employing a Visual Change Index as shown in figure 26.

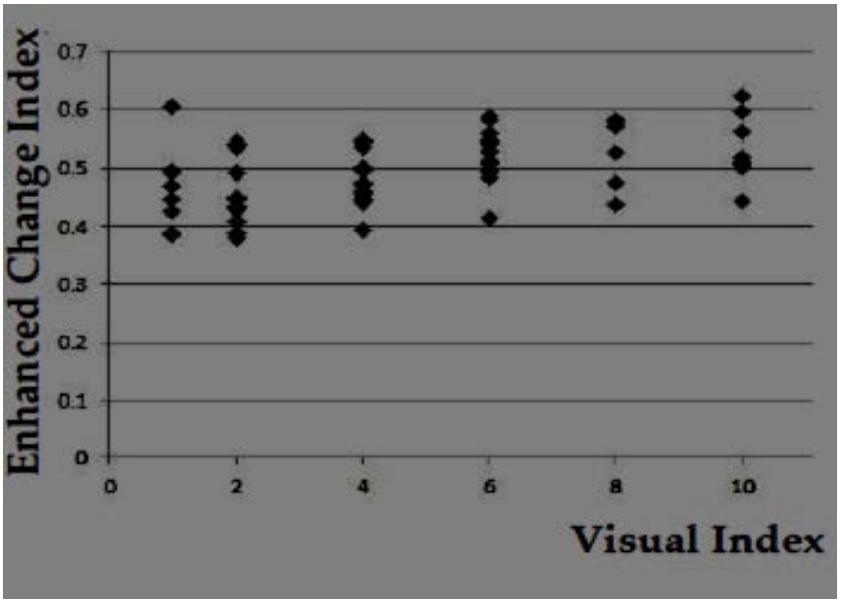

12.

Figure 27 The validation of the calculated Enhanced Change Index validated based on a visual Index obtained for buildings selected random

Potential Applications of Unsupervised Object Based Change Index for High Resolution Images

Unsupervised Building Change Index

The GIS objects pertaining to buildings are used to clip the pre-disaster and post-disaster images. The percentage of change within the buildings is calculated based on the texture, gradient and edges. Figure 28 shows an illustration of the results obtained from running a change detection index of an area pre- and post-disaster. Based on the criteria set for the change index, the algorithm identifies the areas of change and presents the degree of change as shown in legend. To date, the method has only been validated by a visual index.

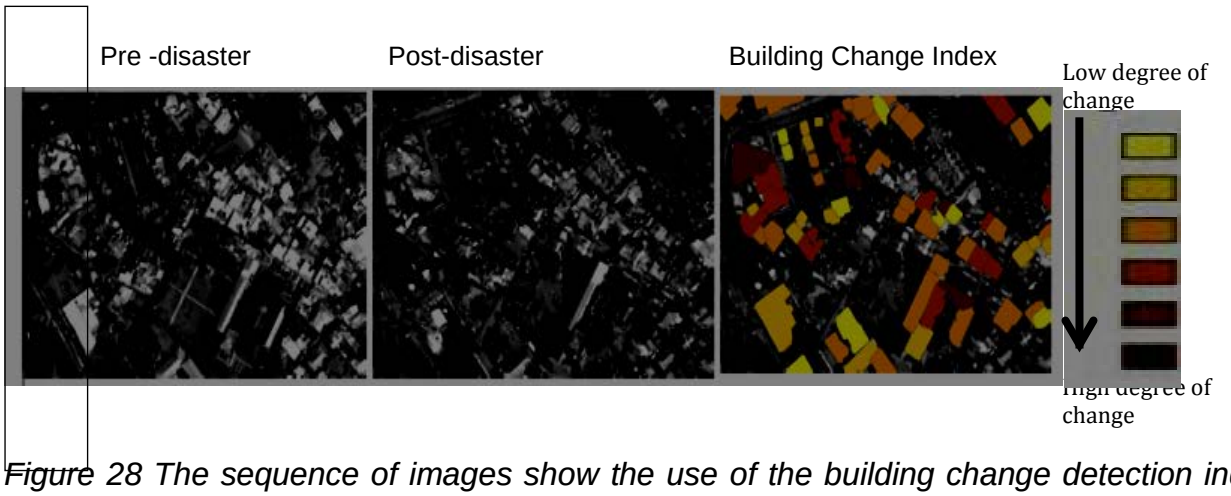

Figure 28 The sequence of images show the use of the building change detection index. The pre and post images are clipped by the GIS objects and the change index is obtained based on the edges, roughness, texture and gradient properties.

For the purposes of SENSUM and especially for WP5 in assessing and monitoring recovery, these maps provide a necessary starting point for focusing on urban areas where the building inventory, its use and density and housed inhabitants may dramatically change in the years after an event such as an earthquake. The ability to assess and monitor these changes, remotely and automatically, may be of significant value to an end-user.
The change detection method for high resolution images can be developed further for other applications in the framework of post-disaster recovery monitoring and assessment (WP5). In the next two sections, two such applications are presented.

Unsupervised Open Areas Change Index

After a disaster in the relief phase, many tents are erected in the available open spaces to house the affected population. Remote sensing techniques can be deployed to identify these open spaces for camps immediately after a disaster, as well as measuring and monitoring recovery. In evaluating two images over a time period, a high level of changes from the previous state (occupied spaces to open spaces again) could imply that the tents have been removed and therefore signify a key milestone in the recovery process. Little change during recovery would imply that few tents have been removed from the open space. Figure 29 shows the use of the change detection index for pertaining the locations of open areas and the level of changes to these plots. The open areas that have changed after disaster are mostly due to the installation of camps and tents. The change over time can show the removal and partial removal of camps. This is helpful to monitor recovery over time.

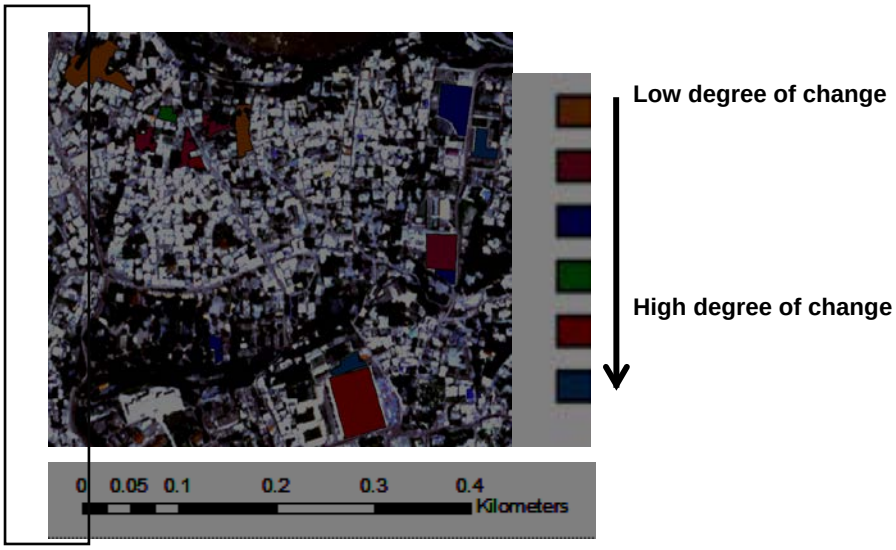

Figure 29 The open area change detection index for Muzaffarabad, Pakistan. The pre and post images are clipped by the GIS objects pertaining to the open areas. The change index is obtained based on the edges, roughness, texture and gradient properties.

Unsupervised Accessibility Change Index

In the same way, the change index technique can be used to help with evaluating and monitoring accessibility in the affected area. Remote sensing data coupled with the increasing availability of road layer information in vector format from OpenStreetMap can be used to assess the percentage of change that has occurred in segments of roads and suggests which roads might have been blocked after the disaster and what percentage of the same roads have undergone a clean-up process during the recovery phase.

This method is based on the assumption that the spectral characteristics of a road which has been blocked by debris and then cleaned up will change abruptly after the disaster and then become more similar to the spectral characteristics of the same road before the disaster. To this end, the workflow has been designed to take segments of roads in the pre-disaster image, and to compare them by means of indices against the same segments in the post-disaster and recovery-time images. In this way, it is easier to have a preliminary and automatic evaluation of how much specific portions of the road network have changed over time. The method, however, is not fully automatic, as change can occur for several reasons. It is therefore for the analyst to verify what has caused the change.

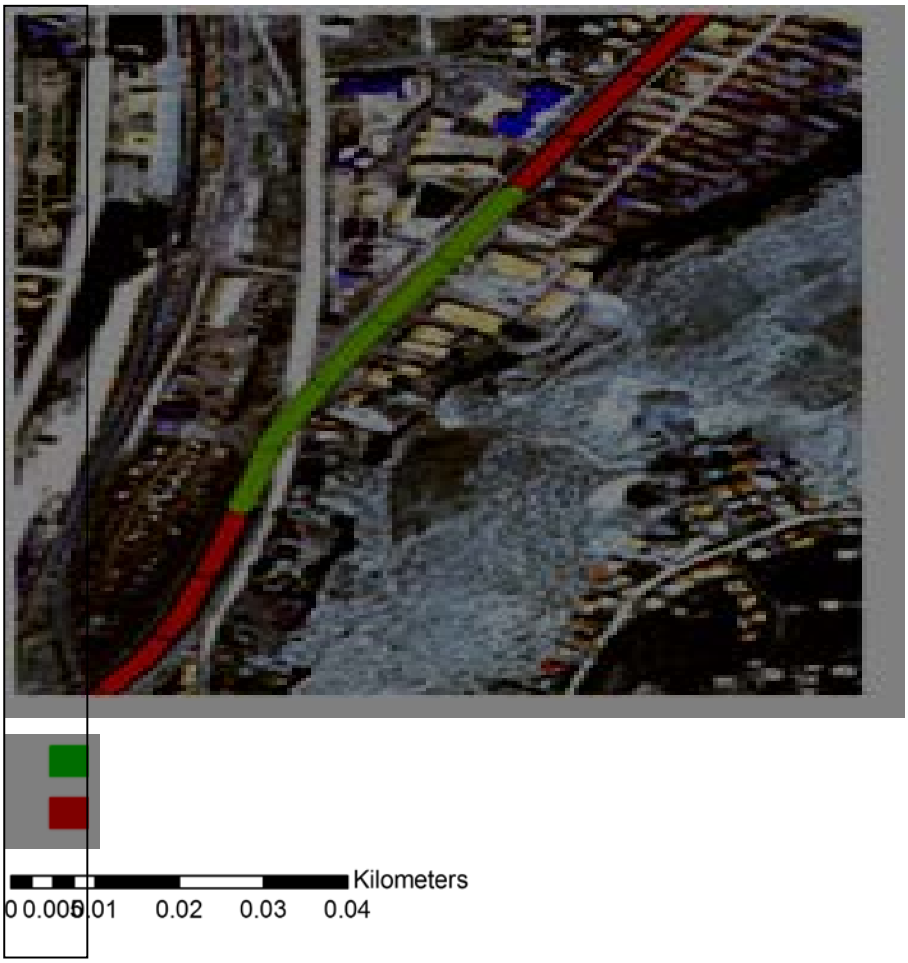

Figure 30 Road change detection index for Van, Turkey. The pre- and post-images are clipped by the GIS objects. The change index is obtained based on the edges, roughness, texture and gradient properties.

Summary

This report presents a review of available methods for supervised and unsupervised change detection for moderate and high resolution images, and methods for co-registration to prepare images prior to running these algorithms. Accurate co-registration of remotely sensed imagery is an important step in time series analysis, data fusion and change detection. All the techniques described require accurately co-registered images in order to produce useful and meaningful results.

Change detection techniques are presented for both medium and high resolution images. For the areas of interest for SENSUM in vulnerability and exposure mapping, medium resolution images would provide temporal information and focus area mapping. For the other intended application of post-disaster recovery monitoring, users would also use temporal analyses to identify focus areas followed by high-resolution data techniques to track specific changes for recovery and building vulnerability analyses.

The proposed SENSUM methods presented in this deliverable will form part of the software development in Deliverable 2.7 and will be tested in the creation of SENSUM products for WP4 and WP5.

References

As-syakur, Abd. Rahman, Wayan Sandi Adnyana, Wayan Arthana and Wayan Nuarsa, (2012) Enhanced Built-Up and Bareness Index (EBBI) for Mapping Built-Up and Bare Land in an Urban Area. Remote Sens. 2012, 4, 2957-2970; doi:10.3390/rs4102957

Bay, H., Ess, A., Tuytelaars, T., Van Gool, L. (2008), "Speeded-Up Robust Features (SURF)", Computer Vision and Image Understanding, vol.110, pp. 346-359.

Boucher, A., Seto, K. C., and Journél, A. G. "A novel method for mapping land cover changes: integrating time and space with geostatistics," IEEE Transactions on Geoscience and Remote Sensing 44(11): 3427-3435.

Calonder, M., Lepetit, V., Stretcha, C., Fua, P., "BRIEF: Binary Robust Independent Elementary Features", 11th European Conference on Computer Vision (ECCV), Heraklion, Crete. LNCS Springer, September 2010.

Chen, X., Zhao,H., Li, P., Yin, Z.,(2006) Remote sensing image-based analysis of the relationship between urban heat island and land use/cover changes. Remote Sensing of Environment 104 (2006) 133–146

Duda, R. O. & Hart, P. E. (1973), Pattern classification and scene analysis, Wiley, New York.

Elmore, A. J., J.F. Mustard, S.J. Manning, and D. B. Lobell, 2000. Quantifying Vegetation Change in Semiarid Environments: Precision and Accuracy of Spectral Mixture Analysis and the Normalized Difference Vegetation Index, Remote Sensing Of Environment, 73:87-102.

Google 2005 http://www.theregister.co.uk/2005/09/07/google_maps_katrina/

Green, K., Kempka, D. & Lackey, L. (1994). Using remote sensing to detect and monitor land cover and land use change. Photogrammetric Engineering and Remote Sensing, 60, 331–337.

Goward, S. N., Masek, J. G., Williams, D. L., Irons, J. R., Thompson, R. J. (2001), "The Landsat 7 mission Terrestrial research and applications for the 21st century", Remote Sensing of the Environment, vol. 78, pp. 3-12.

Gluch, R. (2002). Urban growth detection using texture analysis on merged Landsat TM and SPOT-P data. Photogrammetric Engineering and Remote Sensing, 68, 1283–1288.

Harb, M., De Vecchi, D., Dell'Acqua, F., Iannelli, G. C. (2014), "A Novel Approach in Refining the Geometrical Accuracy of Landsat Images in the context of Temporal Tracking of Built-Up Areas as a Physical Vulnerability Indicator", Submitted to IEEE Transactions on Geoscience and Remote Sensing

Harris, P. M. and Ventura, S. J. (1995). The integration of geographic data with remotely sensed imagery to improve classification in an urban area. Photogrammetric Engineering and Remote Sensing 61, 993–998.

Hung, M., & Ridd, M. K. (2002). A subpixel classifier for urban land-cover mapping based on a maximum-likelihood approach and expert system rules. Photogrammetric

Engineering and Remote Sensing, 68, 1173–1180.

Kaufman, R. K., & Seto, K. C. (2001). Change detection, accuracy, and bias in a sequential analysis of Landsat imagery in the Pearl River Delta, China: Econometric techniques.
Agriculture, Ecosystems and Environment, 85, 95–105.

Li, S., Chen, X., A New Bare-Soil Index For Rapid Mapping Developing Areas Using LANDSAT 8 Data, The International Archives of the Photogrammetry, Remote Sensing and Spatial Information Sciences, Volume XL-4, 2014

Liu J ; Pan Y. ; Zhu X ;Zhu W. (2014) Using phenological metrics and the multiple classifier fusion method to map land cover types. J. Appl. Remote Sens. 8(1), 083691 2014

Jensen, J. R., Cowen, D. C.. Remote sensing of urban/suburban infrastructure and socioeconomic attributes. Photogrammetric Engineering and Remote Sensing, 611–622, 1999.

Lowe, D. G. (2004), "Distinctive Image Features from Scale-Invariant Keypoints", International Journal of Computer Vision, vol. 60, pp. 91-110.

Lucas, R.M., M. Honzak, G. M. Foody, P. J. Curran, & C. Corves 1993, Characterizing tropical secondary forests using multi-temporal Landsat sensor imagery. International Journal of Remote Sensing, 14, 3061-3067.

Lu, D., & Weng, Q. (2005). Urban classification using full spectral information of Landsat ETM+ imagery in Marion County, Indiana. Photogrammetric Engineering and Remote Sensing, 71, 1275–1284.

Main-Knorn , M, W B. Cohen , R E. Kennedy, W Grodzki, D Pflugmacher .P Griffiths , P Hostert
Remote Sensing of Environment 139 (2013) 277–290

Mesev, V.1998. The use of census data for urban image classification. Photogrammetric Engineer-ing and Remote Sensing 64, 431–438.

Myint, S. W. (2001). A robust texture analysis and classification approach for urban land-use and land-cover feature discrimination. Geocarto International, 16, 27–38.

Shaban, M. A., & Dikshit, O. (2001). Improvement of classification in urban areas by the use of tex-tural features: The case study of Lucknow city, Uttar Pradesh. International Journal of Remote Sensing, 22, 565–593.

Stuckens, J., Coppin, P. R., & Bauer, M. E. (2000). Integrating contextual information with per-pixel classification for improved land cover classification. Remote Sensing of Environment, 71, 282–296.

Small, C. (2001). Estimation of urban vegetation abundance by spectral mixture analysis. International Journal of Remote Sensing, 22, 1305–1334.

Small, C. (2001b). Multiresolution analysis of urban reflectance. In: T. Bucciarelli, & O. Hellwich (Eds.), IEEE/ISPRS conference on remote sensing of urban areas. Rome, Italy: IEEE (paper 23).

Singh, A. (1989). Digital change detection techniques using remotely-sensed data. International Journal of Remote Sensing,10, 989–1003.

Stow, D. (1995). Monitoring ecosystem response to global change: multi-temporal remote sensing analyses. In: J. Moreno, & W. Oechel (Eds.), Anticipated effects of a changing global environment in Mediterranean
type ecosystems (pp. 254–286). New York: Springer-Verlag

Taubenböck, H., Esch, T., Felbier, A., Wiesner, M., Roth, A., Dech, S., "Monitoring urbanization in mega cities from space," Remote Sensing of Environment, vol.

117, pp.162-176, 2011.

Thomas, N., Hendrix, C., & Congalton, R. G. (2003). A comparison of urban mapping methods us-ing high-resolution digital imagery. Photogrammetric Engineering and Remote Sensing, 69, 963–972.

Tzimiropoulos, G., Argyriou, V., Zafeiriou, S. (2010), "Robust FFT-Based Scale-Invariant Image Registration with Image Gradients", IEEE Transactions on Pattern Analysis and Machine Intelligence, vol. 32, pp. 1899-1906.

USGS (2014), "Landsat handbook", retrieved online from: http://landsathandbook.gsfc.nasa.gov/sysper/

Vogelmann, J.E., S.M. Howard, L. Yang, C. R. Larson, B. K. Wylie, and J. N. Van Driel, 2001, Com-pletion of the 1990's National Land Cover Data Set for the conterminous United States, Photogrammetric Engineering and Remote Sensing 67:650-662.

Walter, L., G. Hajnóczky. 2005. Mitochondria and endoplasmic reticulum: the lethal interorganelle cross-talk. J. Bioenerg. Biomembr. 37:191–206.

Welch, R. (1982). Spatial resolution requirements for urban studies. International Journal of Remote Sensing, 3(2), 139–146.

Wolter, P.T., Mladenoff, D. J., Host, G. E. & Crow, T. R. (1995). Improved forest classification in the Northern Lake States using multitemporal Landsat imagery. Photogrammetric Engineering and Remote Sensing, 61, 1129–1143.

Xu, H. (2007) Extraction of Urban Built-up Land Features from Landsat Imagery Using a Thematic-oriented Index Combination Technique Photogrammetric Engineering & Remote Sensing Vol. 73, No. 12, December 2007, pp. 1381–1391.

Zitova, B., Flusser, J. (2003), "Image registration methods: a survey", Image and Vision Computing, vol. 21, pp. 977-1000.

Zhang, J., & Foody, G. M. (2001). Fully-fuzzy supervised classification of suburban land cover from remotely sensed imagery: Statistical neural network approaches. International Journal of Re-mote Sensing, 22, 615–628.

Zhang, Q., &Wang, J. (2003). A rule-based urban land use inferring method for fine-resolution multispectral imagery. Canadian Journal of Remote Sensing, 29, 1–13.